63-3-3

ARL 63-15

A FUNDAMENTAL INVESTIGATION OF THE ALLOYING BEHAVIOR OF THE RARE EARTH AND RELATED METALS

J. F. Nachman
C. E. Lundin
A. S. Yamamoto

University of Denver
Denver, Colorado

JANUARY 1963

Aeronautical Research Laboratories
Office of Aerospace Research
United States Air Force

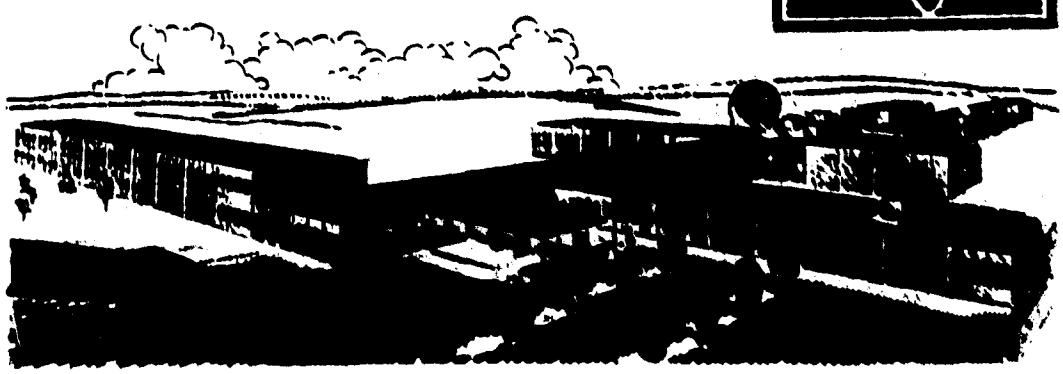

NOTICES

When Government drawings, specifications, or other data are used for any purpose other than in connection with a definitely related Government procurement operation, the United States Government thereby incurs no responsibility nor any obligation whatsoever; and the fact that the Government may have formulated, furnished, or in any way supplied the said drawings, specifications, or other data, is not to be regarded by implication or otherwise as in any manner licensing the holder or any other person or corporation, or conveying any rights or permission to manufacture, use, or sell any patented invention that may in any way be related thereto.

- - - - - - - - -

Qualified requesters may obtain copies of this report from the Armed Services Technical Information Agency, (ASTIA), Arlington Hall Station, Arlington 12, Virginia.

- - - - - - - - -

This report has been released to the Office of Technical Services, U. S. Department of Commerce, Washington 25, D. C. for sale to the general public.

- - - - - - - - -

Copies of ARL Technical Documentary Reports should not be returned to Aeronautical Research Laboratory unless return is required by security considerations, contractual obligations, or notices on a specific document.

AF-WP-L-APR 62 100

25-589, 400, 4-22-63

ARL 63-15

A FUNDAMENTAL INVESTIGATION OF THE ALLOYING BEHAVIOR OF THE RARE EARTHS AND RELATED METALS

J. F. Nachman
C. E. Lundin
A. S. Yamamoto

University of Denver
Denver Research Institute
Denver, Colorado

January 1963

Contract AF-33(616)-6787
Project 7021
Task 7021-01

Aeronautical Research Laboratories
Office of Aerospace Research
United States Air Force
Wright-Patterson Air Force Base, Ohio

FOREWORD

This final technical report was prepared by the Denver Research Institute, University of Denver, Denver, Colorado, on Contract AF 33(616)-6787 for the Aeronautical Research Laboratories, Office of Aerospace Research, United States Air Force. The research described herein was accomplished on Task 7021-01, "Interactions, Imperfections and Alloy Theory" of Project 7021, "Interrelation Between Structure and Properties of Solids" under the technical cognizance of Dr. Lawrence Bidwell of the Metallurgy and Ceramics Research Laboratory of ARL.

The report period is inclusive of 1 November 1959 to 31 October 1962. Messrs. C. E. Lundin and J. F. Nachman were the principal investigators in this research program. Mr. A. S. Yamamoto coordinated the overall experimental phases of the work.

The authors appreciate the counsel of Dr. Rudolph Speiser, Ohio State University and Dr. M. J. Pool, University of Denver. Thanks are due Mr. R. J. McManis for his assistance in the various experimental phases and Mr. Maurice Salmon for the X-ray diffraction analyses. Special appreciation is also due to Mr. Merlyn Salmon, Fluo-X-Spec Analytical Laboratory, Denver, Colorado, for developing the X-ray spectrographic techniques.

ABSTRACT

The vapor pressures of praseodymium, neodymium, and samarium have been measured with a Knudsen effusion apparatus. Also, using the same apparatus, thermodynamic activities of the liquid phase of the praseodymium-neodymium system have been determined. Heats of vaporization were established from the vapor pressure data for praseodymium, neodymium, and samarium. The phase diagram for the praseodymium-neodymium system was determined from thermal analyses, metallographic examinations, and X-ray diffraction studies. Results of the thermodynamic activity studies and measurements of solid (room-temperature) and liquid densities indicate ideal behavior in both liquid and solid solutions, within the experimental error. Ideal behavior was predicted for the praseodymium-neodymium system, as there are essentially no differences between the component elements in considering such variables as electronic structure, crystal structure, atomic diameter, valency effect, electronegativity, and electron concentration.

TABLE OF CONTENTS

TABLE OF CONTENTS (Continued)

LIST OF ILLUSTRATIONS

LIST OF TABLES

LIST OF SYMBOLS

A	cross-sectional area of Knudsen effusion orifice in cm^2
a_i	activity of component i
a_i^l, a_i^v	activities of component i in the liquid and vapor phase, respectively
d	distance between the target and effusion orifice in cm
F°	standard free energy
f	fraction of effusing vapor that strikes the target
f_i	fugacity of component i in the alloy
f_i°	fugacity of the pure component i
H°	standard enthalpy
M	molecular weight
m	condensed mass of the vapor in g
N_i	mole fraction of component i
N_i^l, N_i^v	mole fractions of component i in the liquid and vapor phase, respectively
Pi	vapor pressure of component i in the alloy
P_i°	vapor pressure of the pure component i
p	equilibrium vapor pressure in mm Hg or atmosphere as specified
R	molar gas constant
$R(1)$	Pauling's single-bond radius
r	radius of the target in cm
r'	single-bond covalent radius
T	absolute temperature
t	time in seconds
V	molal volume of the alloy
V_i°	atomic volume of component i
$\overline{V_i}$	partial molal volume of component i
v	Pauling's metallic valence
x	electronegativity
ρ_i	density of component i in g/cc
ρ_A	observed alloy density in g/cc

I. INTRODUCTION

The main objective of this research program is an attempt to establish an understanding of the principles of alloy formation using the rare-earth metals. Because of the slight differences in the basic properties in this transition-metal group, a study of various combinations of binary systems can be systematically undertaken. The variables to be considered are electronic structure, crystal structure, atomic diameter, valency effect, electronegativity, mean Fermi energy, and electron concentration. By appropriate combination of two metals, one can choose a binary system with a minimum number of known, preselected variables. Using two or possibly three property determinations, such as thermodynamic activity, specific volume, density, etc., as criteria of the nature of the system, the effect of each variable can be determined. After a series of systems has been studied, the comparison between each new variable and its effect on the nature of its system under study may lead one to a knowledgeable concept of alloying behavior of the rare-earth metals and possibly, in turn, all of the transition metals. Table I is a summary of the selected rare-earth binary systems to be studied, presenting their constants and variables.

Of the overall objectives which are described above, the first phase has been completed and is reported herein. Briefly the investigations conducted during the past three-year period have been as follows: (1) to design and build a Knudsen effusion apparatus, (2) develop X-ray spectrographic analytical techniques to analyze the rare-earth metal vapor condensates, (3) develop X-ray diffraction, thermal analysis, metallographic, and liquid density techniques to study the rare-earth binary systems, (4) determine the melting points, transition temperatures, and vapor pressures of praseodymium, neodymium, and samarium metals, and (5) determine the thermodynamic activities of the praseodymium-neodymium system. Thus, the first binary system, praseodymium-neodymium, has been successfully completed, and progress on the second binary system, samarium-gadolinium, has been made.

It is noteworthy that the praseodymium-neodymium system which was selected as the system with "no variables" between the two component metals was found experimentally to exhibit essentially complete ideality of the liquid and solid solutions. Referring to Table I, a comparison of the physical characteristics of each component metal shows that praseodymium and neodymium are practically similar in every respect, with the exception of the one electron difference in the 4f electronic shell. However, this difference was expected to be a negligible factor in displacing the ideality of the solution. The near approach to ideality was predicated on the basis of the factors expressed in Table I.

Manuscript released by the authors November 1962 for publication as an ARL technical documentary report.

TABLE I

SELECTED RARE-EARTH BINARY SYSTEMS, THEIR CONSTANTS AND VARIABLES

Structure	Metal	Goldschmidt Atomic Radii	Pauling's Single-Bond Radii	Mean Fermi Energy	Valence	Electro-negativity	Variables	Constants
HCP, abcb	Nd	1.82	1.64	4.32	3	1.26	None	Valence
HCP, abcb	Pr	1.83	1.64	4.29	3	1.26		Valency Effects Electronegativity Atomic Diameter Mean F. E. Electronic Structure Crystal Structure Electron Concentration
Rhomb.	Sm	1.80	1.62	4.41	3	1.26	Crystal	Electronegativity
HCP-A3	Gd	1.80	1.62	4.41	3	1.26	Structure	Valence Valency Effects Atomic Diameter Mean F. E. Electronic Structure Electron Concentration
HCP-A3	Y	1.81	1.62	4.42	3	1.27	Electronic	Electronegativity
HCP-A3	Gd	1.80	1.62	4.41	3	1.26	Structure	Atomic Diameter Mean F. E. Crystal Structure Electron Concentration

TABLE I (Cont'd)

Structure	Metal	Goldschmidt Atomic Radii	Pauling's Single-Bond Radii	Mean Fermi Energy	Valence	Electro-negativity	Variables	Constants
HCP-A3 Rhomb.	Y	1.81	1.62	4.42	3	1.27	Electronic Structure	Valency Effects
	Sm	1.80	1.62	4.41	3	1.26	Crystal Structure	Electronegativity
								Atomic Diameter
								Mean F. E.
								Valence
								Valency Effects
								Electron Concentration

Since the praseodymium-neodymium system was experimentally established to exhibit essentially ideal conditions in both the liquid and solid solutions, the hypothesis set forth in the overall objectives is confirmed in this first phase. The study of subsequent systems where variables are introduced by proper selection of the component metals now becomes more meaningful.

II. SCIENTIFIC BACKGROUND

It has long been recognized that because of a slight gradation in properties, the rare earths, or lanthanons, (atomic numbers 58-71) have been extremely difficult to separate from one another by ordinary chemical means. However, from the metallurgical viewpoint this slight gradation in properties can be of considerable interest. In surveying the properties of the lanthanons, a very interesting and significant fact becomes apparent. It is found that the properties, in general, are approximately a linear function of the atomic number, with the exception of europium and ytterbium. A plot of interatomic spacing versus atomic number shows a linear decrease in interatomic distance with increasing atomic number, indicating a strengthening of the atomic bond in the elements of higher atomic numbers. This is manifested in the following ways:

(a) An approximate linear increase in melting point and Young's Modulus[1] with increasing atomic number.

(b) An approximate linear decrease in compressibility[1] with increasing atomic number.

Notable exceptions to the above are europium and ytterbium, in some instances, cerium. These anomalies may in part be traced to a difference in crystal structure. Most of the lanthanons appear to crystallize in the hexagonal system, while cerium, europium, and ytterbium exhibit a face-centered cubic, body-centered, and face-centered cubic room-temperature structure, respectively.

A plot of Pauling's[2] single-bond metallic radii versus atomic number exhibits a similar linear relationship, with the exception of europium and ytterbium (Figure 1). This is attributed to the fact that most of the lanthanons have a metallic valence of 3, whereas europium and ytterbium have metallic valences of 2. In this respect, europium and ytterbium more closely resemble the alkaline earths than the rare earths. Note that in Pauling's plot in Figure 1 a straight line can be drawn connecting barium, europium, and ytterbium. Further evidence of this similarity is provided by the work of Spedding, et al.,[3] which indicates that both europium and ytterbium are very soft and ductile, bearing closer resemblance to the alkaline earths than to the lanthanons. Resistivity measurements also show that europium and ytterbium are similar in this property to their isostructural counterparts, barium and strontium. These same investigations show that the melting points of europium and ytterbium are in the same temperature range as the alkaline earths. These observations perhaps do not appear too surprising, when it is considered that the straight-line portions of Pauling's curves indicate a constancy in valence and bonding types.

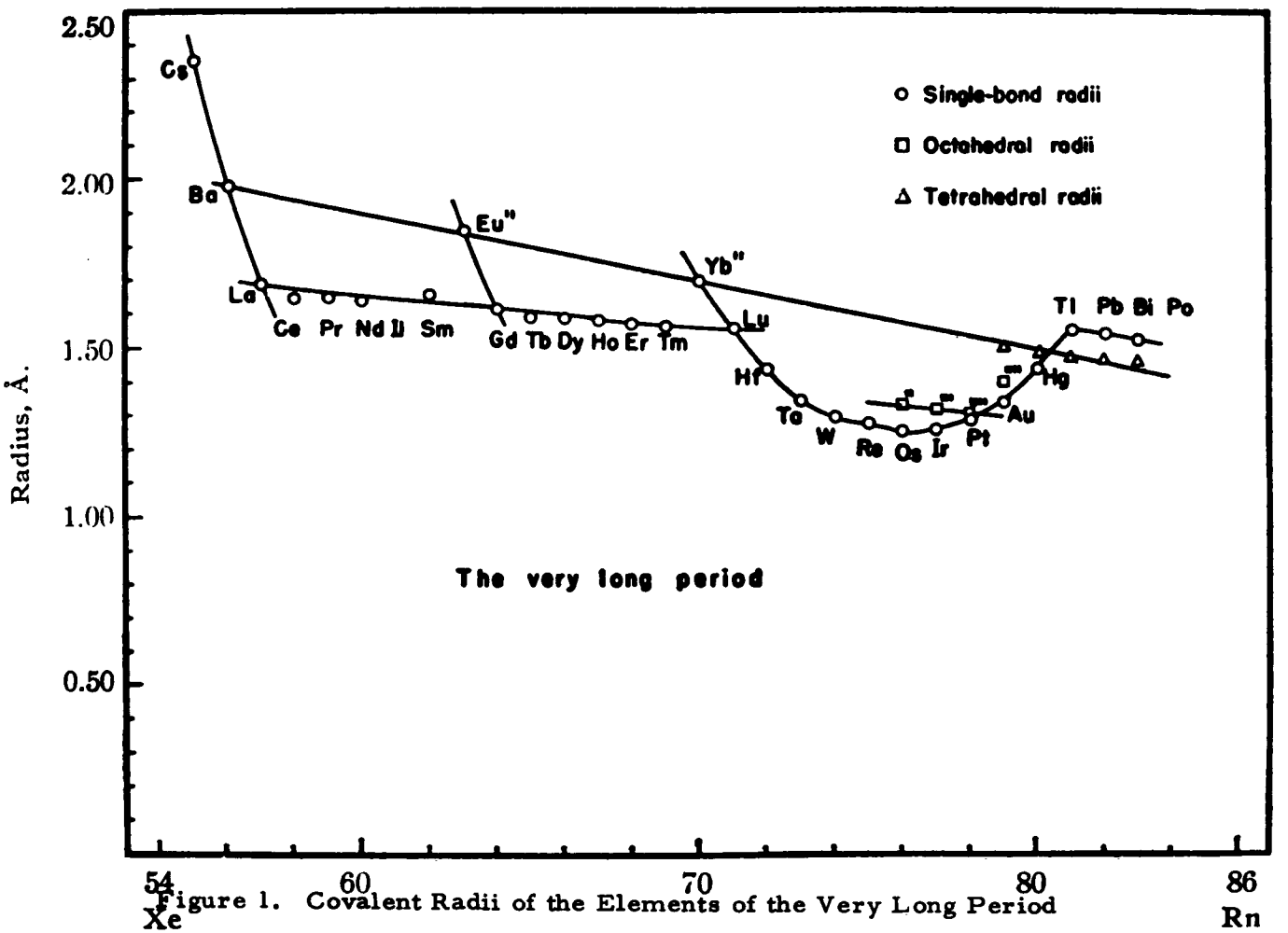

Figure 1. Covalent Radii of the Elements of the Very Long Period

As one would expect, the electronegativity variation across the rare-earth series is negligible. The electronegativities of the lanthanons listed in Table II were derived from Gordy's relation[4]

$$x = 0.31 \frac{n' + 1}{r'} + 0.50,$$

where n' = valence electrons and r' = single-bond covalent radius, and x = electronegativity in units of the square root of electron volts per bond. Pauling's metallic valence v, and covalent single-bond radius R(1) were substituted for n' and r', respectively, in the above expression. Values for v and R(1) are listed in Table II. Note that, with the exception of europium and ytterbium, the electronegativities are approximately constant and equal to 1.3. The alkaline earths, barium and strontium, are included for purposes of comparison. Again, the similarity of europium and ytterbium to the alkaline earths is emphasized.

Based upon the Goldschmidt atomic diameter C.N. 12, the size-factor difference for most of the lanthanons lies well within the widely accepted value of 15 percent required for solid solubility. The greatest size-factor difference occurs between the elements europium (4.08A) and lutetium (3.47A), and may represent a borderline case. If one considers the transition metal pairs of Group III and Group IV--namely, Sc-Ti, Y-Zr, and La-Hf, one finds that a constant electronegativity difference of about 0.3 exists. These data are presented in Table II. However, the pair, La-Hf, has a unique group of thirteen metals, the lanthanons, interposed.

In summing up, then, one might consider the total variation in properties across the rare-earth series as representing the gross difference in properties between lanthanium and hafnium, elements which are found adjacent to one another in the periodic table. Effectively, we have been provided with the ability to interpose between these two elements, thirteen subtransition elements exhibiting a gentle gradation in properties, and whose properties are essentially a linear function of the atomic number.

For the reasons stated above, it is felt that the rare-earth series form a logical basis for a fundamental study of the alloying behavior of the transition metals.

TABLE II

ATOMIC PROPERTIES OF RARE-EARTH ELEMENTS AND OTHERS

At. No.	Element	Pauling's Metallic Valence, v	Pauling's Single-bond Radii, R(1)	Electronegativity, x
57	La	3	1.690	1.24
58	Ce	3.2	1.646	1.29
59	Pr	3.1	1.643	1.26
60	Nd	3.1	1.637	1.26
61	Pm	3	1.633	1.26
62	Sm	2.8	1.623	1.26
63	Eu	2	1.850	1.00
64	Gd	3	1.623	1.26
65	Tb	3.5	1.613	1.37
66	Dy	3	1.600	1.28
67	Ho	3	1.581	1.28
68	Er	3	1.580	1.28
69	Tm	3	1.578	1.29
70	Yb	2	1.699	1.05
71	Lu	3	1.557	1.30
72	Hf	4	1.44	1.57
38	Sr	2	1.914	0.99
56	Ba	2	1.981	0.97
29	Sc	3	1.439	1.36
22	Ti	4	1.324	1.67
39	Y	3	1.616	1.27
40	Zr	4	1.454	1.57

III. EXPERIMENTAL

A. KNUDSEN EFFUSION APPARATUS

The activities of the components of the binary alloys were determined from the partial pressure of the vapor in equilibrium with the alloy. The experimental procedures described by Speiser, Jacobs, and Spretnak[5] were employed, although the Knudsen effusion apparatus was a modified version.

Since the literature survey revealed vapor-pressure data for praseodymium metal only, the determination of the vapor pressures of neodymium and samarium metals was imperative before the binary systems could be studied. Therefore, an analytical balance was incorporated in the apparatus to conduct a quantitative measurement of the weights of the condensed vapors.

Another modification was the use of resistance heating instead of induction heating. The advantage of resistance heating is that better control of the temperature of the effusion cell is obtained. Also, more accurate temperature measurement is achieved through use of a thermocouple.

Figure 2 shows a general view of the assembly. The apparatus consists of three major parts; a heating chamber, analytical balance, and vacuum system.

1. The Heating Chamber and Internal Components

(a) Heating and temperature control. The heating chamber is suspended underneath a one-inch thick duralumin base-plate at the left-hand side upon which an analytical balance is mounted (See Figure 2). The dimensions of the chamber are 4 inches ID × 12 inches long. The steel cylinder is water-cooled by means of 1/4 inch OD copper tubing wrapped around the shell. The stainless-steel bottom plate has a pair of sealed, high-voltage terminals for the electrical connections to a tungsten heating coil. A number of terminals are also provided for thermocouples in the center of this plate. The design of the plate can be seen at the extreme right in Figure 3. In the picture, all the components situated in the heating chamber are shown in the following order: a stainless-steel tripod, tantalum bottom shield with three tantalum prongs, tantalum effusion cell, tungsten heating coil, and tantalum side and top thermal shields.

The tungsten heating coils, made of three-stranded, 0.055 inch wire, were purchased from General Electric Company. Their dimensions are 0.950 inch in diameter × 1-1/4 inches in height, having approximately 9-1/2 turns. The coils are heated by an electrical potential from a source capable of providing 570 amp at 15.3 v. The source consists of a series of three step-down transformers. The current through the tungsten coils is varied by means of a Variac transformer until the desired temperature is reached.

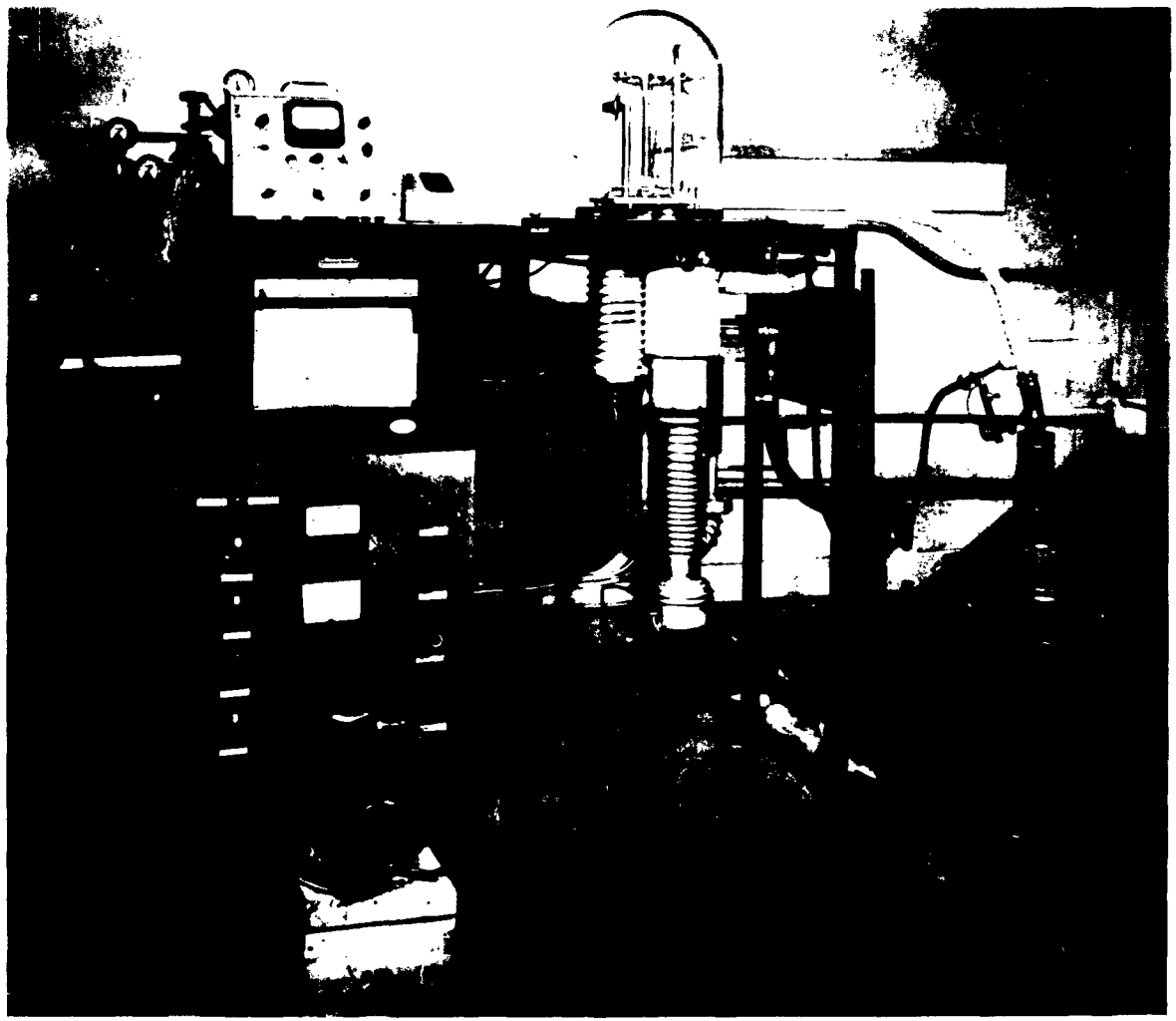

Figure 2. General View of the Knudseon Effusion Apparatus

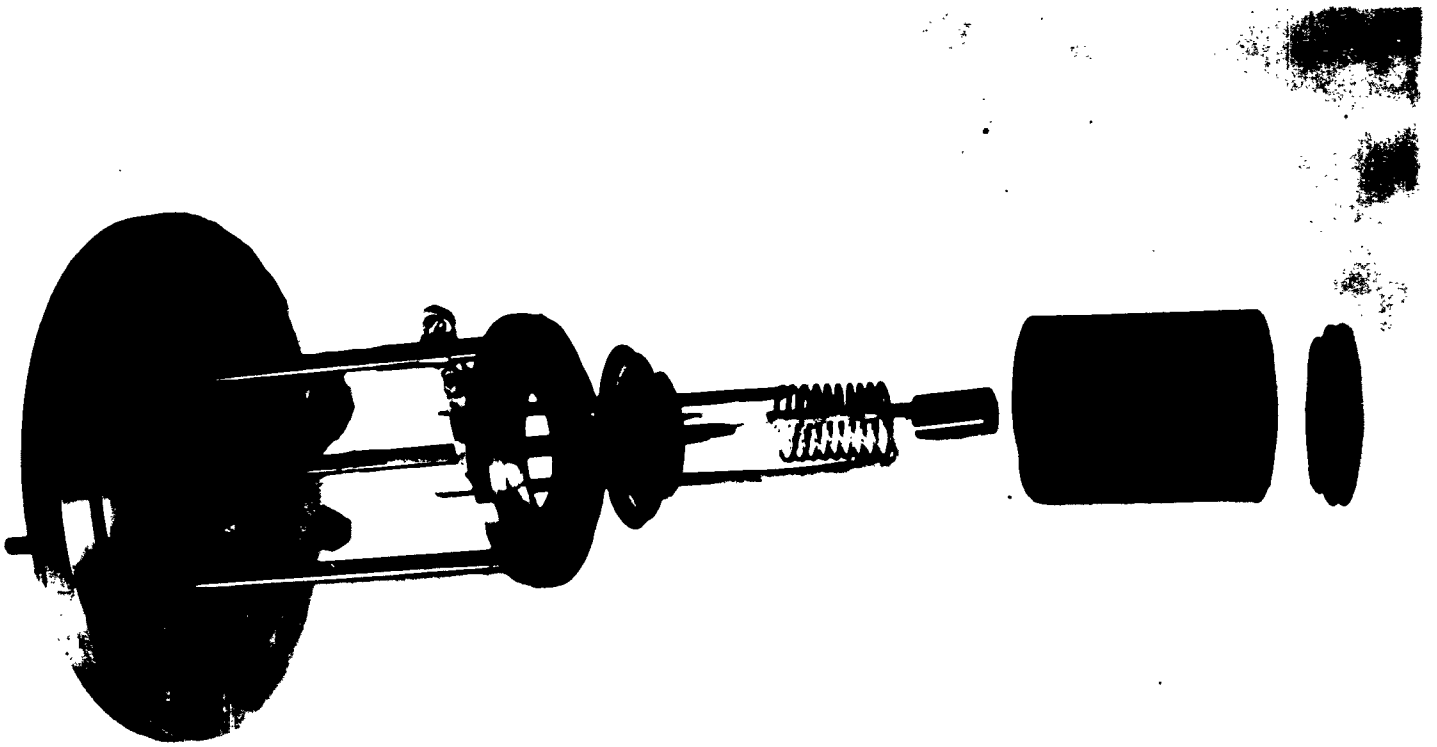

Figure 3. An Exploded View of Knudsen Effusion Cell and Heating Components

The condensation of vapor on the underside of the effusion cell lid can be prevented by raising the temperature in the vicinity of the lid slightly higher than the rest of the crucible. This was achieved by bringing the top two or three turns of the coil closer with a pair of the coil spacers and by positioning the effusion cell lid at this level. The spacers were made of high-purity alumina.

Further control at temperature is accomplished with a Minneapolis-Honeywell, Brown Electronik recorder-controller with an off-on operation of a single-point contactor in series with the one leg of the primary circuit of the transformers.

(b) Effusion cell. Tantalum was chosen as the material for the effusion cells in view of earlier investigations conducted at the Ames Laboratory, Iowa State University,[6] which reports the metal as highly resistant to alloying with the rare-earth metals at temperatures up to 1500°C.

The final design for the tantalum effusion cells resulted from a series of changes which were made earlier in the investigation. Figure 4 illustrates the cell design which was used in obtaining the major portion of the data reported herein. As can be seen, the cell consists of four pieces, the main body (13/16 inch long × 1/2 inch OD × 0.015 inch wall), thermocouple well (9/32 inch long × 3/16 inch OD × 0.010 inch wall), lid, and bottom. Thin walled tantalum tubing of the two different sizes and rod of 1/2 inch in diameter were purchased from the Kawecki Chemical Company.

The thermocouple well is made by crimping one end of a piece of 3/16 inch OD tube to an edge, seam welding it, and finally welding circumferentially onto the bottom section. This subassembly is welded to a 1/2 inch OD tube to complete the crucible and is then leak checked. All of the welding operation is conducted in a chamber which is dynamically purged with helium gas in addition to the inert atmosphere provided through a Heliarc welding electrode.

This design allows the placement of the thermocouple tip in the center of the contained liquid or solid metal, separated only by a thin-walled tantalum protection tube. Measurement of temperature of the contents of the cell is extremely sensitive. Therefore, it is possible to use the apparatus to accurately determine the melting points and phase transformations in the pure rare-earth metals, and the liquidus, solidus, and transformation temperatures of the binary alloys. Thus, both vapor-pressure data and phase-diagram determinations can be obtained with this technique.

Circumferential welding of the lid onto the effusion cell was necessary because of the creeping of the rare-earth metal up the side walls of the cell and through the crevice between the lid and the cell. No problem was observed with the pure silver and copper metals during temperature calibration and during

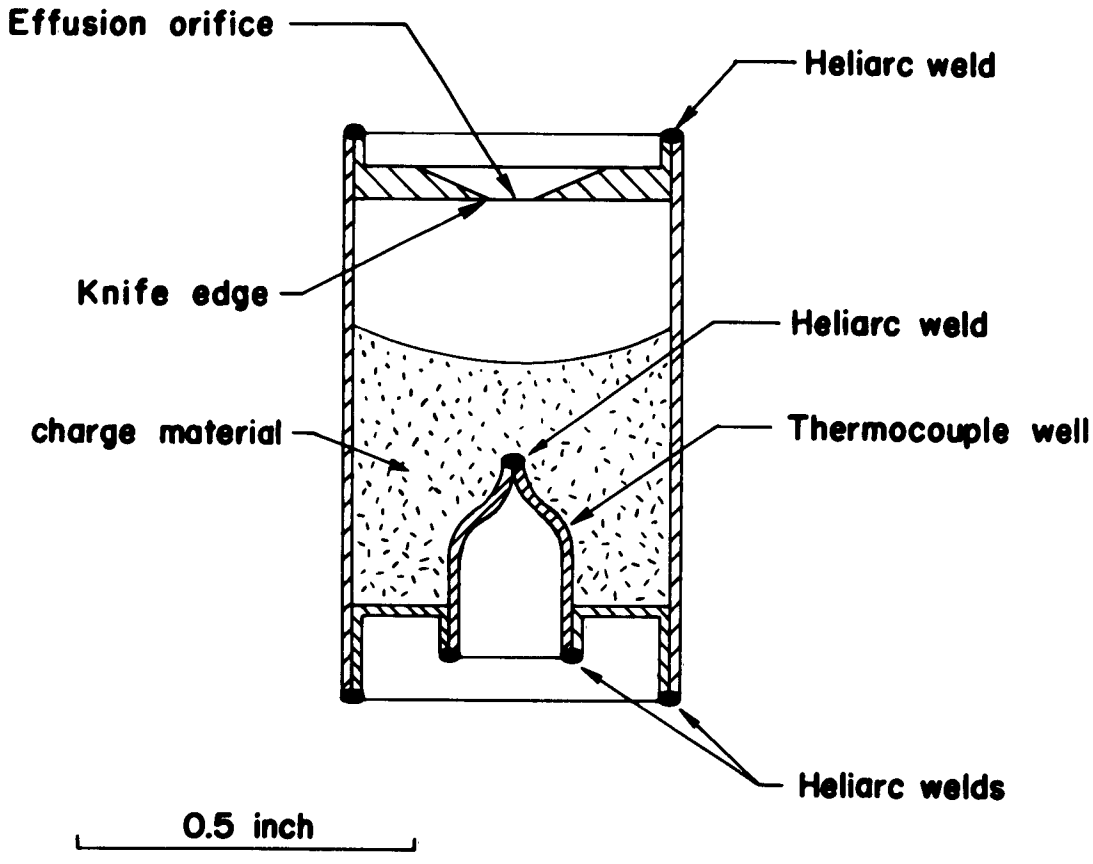

Figure 4. Effusion Cell Design

vapor-pressure determinations of pure silver. Apparently, however, the rare earths wet the tantalum much easier than the above metals. The loss of vapor out the edge of the lid would cause serious errors in vapor-pressure measurement. An attempt was made to seal this gap by machining the lid oversize and forcing it into place. The plan was to heat the cell below the melting point of the charge inside and allow solid-state diffusion bonding to occur before carrying on subsequently with the vapor-pressure measurements. This technique did not effectively seal the lid to the cell. Therefore, the welding of the lid to the cell wall was necessary. The welded design is accomplished by machining a lip on the lid to match a lip on the cell wall. The closure is made by fusing the two lips together around the top periphery of the cell. Since the charge material has to be placed in the cell before welding the lid, a special welding technique was developed to prevent heating and oxidation of the charge. The problem of welding is particularly acute with rare-earth charges, because they oxidize so easily when heated. Therefore, a special holding jig was developed to keep all but the localized zone near the weld cold. The jig consists of a close-fitting copper cylinder into which the tantalum cell is placed so that only the lip extends above a heavy copper plate. The plate and the cylinder walls are water-cooled by means of a water jacket surrounding the inner cylinder. A gentle flow of helium is maintained from below the cell. This entire assembly is also placed into the chamber described above. The welding of this and the other two seams is done with a Heliarc torch with a very small amperage.

(c) Thermal shields. A series of experiments and subsequent improvements in design resulted in the thermal shielding assembly described below. Very little heat loss was observed with the assembly of this final design. This also facilitated easier loading and unloading of the effusion cell. Chemical cleaning of vapor depositions from the assembly was handled easily and effectively due to inertness of tantalum to acids.

The thermal shielding assembly, approximately 2 inches in height × 2 inches in diameter, consists of the three separable parts; the cover, side and bottom shields. (See Figure 3). Each part is made of three layers of 0.005 inch thick tantalum sheet spaced by 1/8 inch tantalum fastener pins. The opening in the cover shield decreases successively from the topmost to the bottom layer. The bottom or support shield is provided with three tantalum pins which position the effusion cell in the hot zone of the heater element. These pins are tapered at the ends to points to reduce the contact area with the effusion cell to a minimum. The thermocouple and power leads are brought through the bottom shield by close-fitting holes.

This whole assembly is placed onto the stainless steel tripod. The effusion cell, thermal shields, and tripod are designed so that they would align very close with the center line of the heating chamber and consequently with the target, which is suspended 10 cm above the effusion orifice.

(d) Thermocouple. In general, the most serious error in determining vapor pressures is in the measurement of the temperature. The use of a thermocouple instead of an optical pyrometer for temperature measurement in this specific application has many advantages. Since the Knudsen effusion cell has proved to function extremely well as a thermal analysis tool, this feature has provided valuable phase-equilibrium data in addition to the activity data. The technique also offered a means to internally standardize the temperature measured in each run in the apparatus, if necessary.

McCabe and Birchenall[7] report that, in their study of the vapor pressures of silver, the diameter of the thermocouple wire can affect the accuracy of the temperature measurements. In their earlier work[8] they observed melting temperatures of the material 10 to 15°C lower than the accepted value due to the heat conduction through the thermocouple. After plotting the varying diameters of the thermocouple versus the observed temperatures, the accepted melting point of silver was attained by extrapolating the thermocouple wire diameter to zero size. Thus, in determination of vapor pressures and activities, thermocouple wires of 0.005 inch in diameter were used.

Temperature measurements with a platinum/platinum-13 percent rhodium thermocouple in the Knudsen effusion cell were satisfactory up to 1200°C in the presence of silver vapor. However, thermocouples of this type were easily contaminated with the vapors of the rare-earth metals. For the study of the praseodymium-neodymium alloy system, it was desirable to seek better means of temperature measurement at these high temperatures. Recent advances[9] in the development of high-temperature thermocouples indicated that tungsten/rhenium and molybdenum/rhenium thermocouples were worthy of consideration for use in this specific application. The reliability of tungsten/rhenium thermoelectric material has been verified in development programs carried on at the General Electric Company, Aircraft Nuclear Propulsion Department and the Minneapolis-Honeywell Research Center. These researchers report that tungsten/rhenium thermocouples are useful up to 4000°F (2204°C) and demonstrate good reproducibility. Accurate calibrations now exist for both of these thermocouple types. Therefore, it was decided to try tungsten/rhenium thermocouples for control and measurement of the temperature in the effusion cell. However, these thermocouples were found to alter slightly their thermoelectric characteristics after a prolonged time at elevated temperatures. After experimenting with the tungsten/rhenium thermocouples, a second type, i.e., tungsten/tungsten-25 percent rhenium couples were employed. The latter thermocouples are reported to be much more stable thermoelectrically at the elevated temperatures than the former. The tungsten/tungsten-25 percent rhenium thermocouple wire, 0.005 inch in diameter, was purchased from Chase Brass and Copper Company.

Even though this thermocouple exhibited a greater stability of thermoelectric characteristics than the tungsten/rhenium couple, a slight shift in

thermoelectric properties was noted to occur after repeated use at the high temperatures. It was concluded that this problem could be eliminated by fully recovering the cold-worked structure in the thermocouple wires prior to their use. A heat treating procedure was, therefore, devised whereby it would be possible to induce a fully recovered structure in the thermocouple subsequent to its proper installation in the thermocouple well of the tantalum effusion cell. This procedure consists of passing a current of 1.5-1.6 amp at 16-18v through the thermocouple wires for approximately 20 minutes. Heating for periods of time up to 1-1/2 hour does not alter the thermoelectric characteristics, indicating that stability is achieved after annealing for 20 minutes. To improve the heat transfer from the crucible to the thermocouple, the thermocouple bead was welded to the wall of the thermocouple well by arc-discharge of a bank of condensers through the thermocouple wires. During the run, vibration was apparently causing the thermocouple to open because of the brittle nature of the bead. A bead was formed by brazing a platinum wire around the junction in an attempt to eliminate this difficulty, but because of the embrittling effect of the rare-earth metal vapors upon the platinum, this bead also failed. The problem was eventually solved by using a tantalum-brazed bead, which was then welded to the tantalum effusion cell by an arc-discharge from a bank of condensers as mentioned above. This brazing operation produces a more ductile bead.

A calibration of the tungsten/tungsten-25 percent rhenium thermocouples with the tantalum bead was carried out against a standard platinum/platinum-13 percent rhodium thermocouple which was checked against the melting points of pure metals. The tungsten/tungsten-25 percent rhenium couple was welded adjacent to the standard thermocouple in a well drilled into a solid tantalum cylinder of approximately the same size as a Knudsen effusion cell, given a recovery anneal as described above, and calibrated in the Knudsen effusion apparatus over a temperature range of 700 to 1550°C. The estimated accuracy of the tungsten/tungsten-25 percent rhenium thermocouple is ± 5°C over a temperature range of 1400 to 1550°C.

The curve for converting from measured millivolts to degrees centigrade for the tungsten/tungsten-25 percent rhenium thermocouple of a particular lot was plotted using the data obtained as described above. These data points were supplemented with the melting temperature of pure silver and copper employing the double thermocouples, platinum/platinum-13 percent rhodium and tungsten/tungsten-25 percent rhenium.

(e) Temperature calibration of Knudsen effusion apparatus. In this investigation an accurate measure of the temperature was a vital factor in the determination of valid vapor pressures and activities. Early in the course of the research effort, it was decided to determine the vapor pressure of silver with the Knudsen effusion apparatus as a calibration of its operation. Silver

was chosen because its vapor pressure has been well established and could be considered a good primary standard with which to compare. During the calibration procedure with silver, it was found that the melting and freezing points of silver were well defined by thermal arrests in the heating or cooling curves on the chart of the temperature recorder-controller. However, the first experiments indicated a sizable correction between the measured and the standard temperature. Modifications of the equipment were then undertaken to correct this situation. The modifications, as described elsewhere in this report, resulted in a very small temperature difference. In addition, the temperature of the thermal arrest remained constant until freezing or melting was complete which indicated that the thermocouple was in intimate association with the sample. The use of a thermocouple in this particular application had several important advantages, as follows:

1. Temperature calibration of the apparatus with high-purity metals of known melting points was accurately established.
2. Thermal analyses of the alloys were conducted to provide liquidus, solidus, and phase transformation temperatures to construct the phase diagrams.
3. Integrity of the thermocouple was checked after a vapor-pressure determination was made to provide assurance that the data were valid.

Temperature calibration was conducted using copper and silver. The data which are presented below show excellent agreement with the literature values.[10]

	Ag	Cu
Measured Melting Temperature, °C	960.2	1079.3
Reported Melting Temperature, °C	960.8	1083.0

(f) Accessories. Various accessories have been designed and constructed for use in conjunction with the vapor pressure and activity measurements.

The target which was used in the calibration of the Knudsen effusion apparatus with high-purity silver was a sterling silver disc, 3 inches in diameter and 0.050 inch thick. Another target was designed for the activity measurements with the rare-earth metals. This was a platinum-10 percent iridium target of the same size. The platinum-iridium target material was selected because of the need for a target inert to the nitric acid which was used to dissolve the rare-earth condensate. To allow for ease in immersing the platinum-iridium target, a brass target holder was designed and constructed to release the target disc with a simple adjustment. The target can then be remounted after dissolving the condensate.

Since the target-to-orifice distance is a factor which has to be known before calculating the vapor pressure, an accurate measurement of this distance must be made during each loading. The poor accessibility of the target and effusion cell once this apparatus is assembled in the furnace chamber does not allow easy measurement. Therefore, a means of measuring this distance before assembly was developed. Since the effusion cell is supported from the furnace base plate, the measurement is made relative to it. To preset the required orifice-to-target distance, several accessory devices were designed and built to obtain the distance accurately. A level-surface plate in conjunction with a height gage were employed to conduct the measurement. The furnace base plate and the assembled effusion apparatus are mounted on the level-surface plate. The height gage is used to determine the height of the orifice above the base plate. Then, an adjustable pedestal, incorporating this height plus the target-to-orifice distance, is used to obtain the final desired target-to-orifice distance. This measurement is made within ± 0.001 inch.

A spark-discharge device was constructed for welding the fine thermocouple wires used to measure and control the temperature in the effusion cell. The operation of the device is based on the discharging of a bank of condensers which are charged by a DC power rectifier source. The thermocouple tips are twisted and used as one electrode, and a copper bar is used as the other electrode.

2. Balance

The balance, shown in Figure 5, was specially designed and constructed to determine the vapor pressures of the pure components, although these data were not specified contractually. Most of the parts for the balance were purchased from Ainsworth & Sons, Inc., Denver, Colorado. Every precaution was taken so that degassing from any part of the balance assembly would be minimized. The sensitivity of this analytical balance is 0.1 mg.

Since the balance is in the vacuum system, the controls are designed to be transmitted through the base-plate by means of two control rods. One control (see the left knob protruding from underneath the base-plate in Figure 2) is to release the beam from its locked position, as well as to move the specially designed pan-arrest from underneath the pans, while the other (the right knob) is to adjust the chain weight during the experiment. The chain weight ranges from 0 to 100 mg. The weights of the vapor condensates of the experimental metals are contained within the limit of the chain weight. Therefore, it is possible to measure weight gains of the target as condensation takes place continually by simply manipulating the control rod to the chain, without breaking the vacuum.

There is also another control rod to equilibrate the balance after the target is suspended and counter-weighted, but before the bell jar is placed over

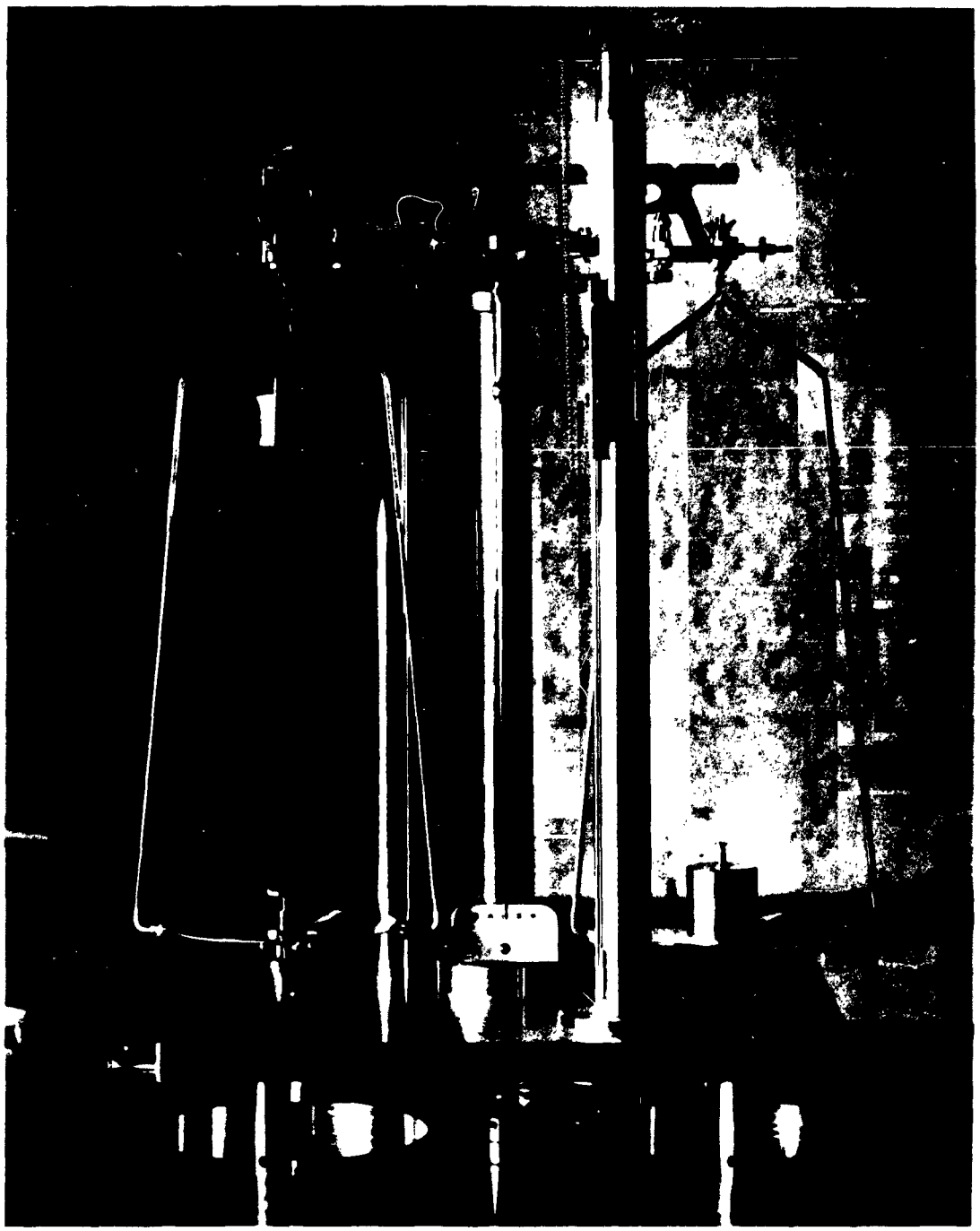

Figure 5. Close-Up View of Balance

the assembly. The dimension of the bell jar is 18 inches in height × 12-1/2 inches in diameter.

The target is suspended with a fine tungsten wire from the bottom of the left pan through a small hole in the platform which supports the structure of the balance. The fixture on the left pan is designed to allow adjustment of the vertical position of the target in the heating chamber.

3. Vacuum System

The vacuum system for the Knudsen effusion apparatus consists of a Model 1402B, Duo-Seal vacuum pump (manufactured by Welch Scientific Company), an MCF-300, fractionating diffusion pump (manufactured by Consolidated Electrodynamics Corporation), and a liquid-nitrogen cold trap. The cold trap is provided to prevent the oil vapor from the oil-diffusion pump from entering the upper system.

A National Research Corporation Type 507 ion gauge and a Type 501 thermocouple gauge are attached toward the upper end of the cold trap for the measurement of the degree of vacuum.

The quality of vacuum in the Knudsen effusion technique is important, especially when using the target method and reactive metals, such as the rare earths. The assembled equipment as seen in Figure 2 was carefully leak checked with a helium leak detector to reduce the air leakage to the absolute minimum. The vacuum obtainable is 9×10^{-8} mm Hg when the heating unit is cold and 1.5×10^{-7} mm Hg while operating at a temperature of 1550°C.

B. MATERIALS

The parameters considered useful in the study of the alloying behavior among the rare-earth metals were vapor pressure, thermodynamic activities, density, phase equilibria, and precise lattice parameters. The procurement of the desired metals of the highest purity available, therefore, was imperative. Praseodymium, neodymium, gadolinium, and samarium of special high-purity grade were purchased from the Ames Laboratory, Iowa State University, Ames, Iowa. The chemical analyses of these special metals furnished by the supplier are tabulated in Table III.

A quantity of 99.9999 percent silver was obtained from the Consolidated Mining and Smelting Company of Canada Limited, Montreal, Canada. Also, spectrographically standardized copper was purchased from Johnson, Matthey, and Company, Limited. The total metallic impurities were reported to be less than 13.5 ppm. Both metals were used to calibrate the Knudsen effusion apparatus.

TABLE III

CHEMICAL ANALYSES OF RARE-EARTH METALS OF SPECIAL HIGH PURITY FURNISHED BY AMES LABORATORY

Impurity	Pr	Nd	Sm	Gd
C	65 ppm	62 ppm	30 ppm	150 ppm
N	50 ppm	39 ppm	< 25 ppm	100 ppm
O	-	-	-	-
F	27 ppm	200 ppm	< 17 ppm	800 ppm
Ti	-	-	-	-
Fe	-	0.01%	0.002%	0.01%
Y	-	-	VW	-
La	$\leq$0.005%	-	-	-
Ce	$\leq$0.1%	-	-	-
Pr	-	$\leq$0.08%	-	-
Nd	~0.06%	-	$\leq$0.02%	-
Sm	-	< 0.06%	-	-
Eu	-	-	$\leq$0.01%	-
Gd	-	-	$\leq$0.01%	-
Tb	-	-	-	-
Dy	-	-	-	-
Ho	-	-	-	-
Er	-	-	-	-
Yb	-	-	VFT	-
Ca	<0.02%	<0.03%	0.05%	<0.005%
Si	< 0.025%	< 0.025%	-	<0.025%
Mg	< 0.01%	< 0.01%	-	$\leq$0.02%
Ta	~0.05%	0.05%	-	<0.05%
Remarks	No other rare earth metals were detected	No other rare earth metals were detected	-	No other rare earth metals were detected

C. PREPARATION OF ALLOYS

The as-received ingots of rare-earth metals were cut into smaller pieces with a jeweler's saw to keep the cutting loss to a minimum. These pieces were used to weigh the alloy charges for subsequent arc melting. Alloy charges were weighed to the nearest 0.1 mg. The total charge-weight of each composition was approximately 20 g. A total of nine alloy charges were prepared at 10 atomic percent increments. Also, pure metals were prepared for melting. Immediately prior to weighing, the pieces were surface filed to remove the surface contamination. The weighing was conducted as rapidly as possible and each charge was then placed into the arc furnace, which was immediately evacuated to prevent any further surface contamination.

Arc melting was accomplished in a standard non-consumable electrode arc furnace in a purified atmosphere of argon. The ingots were inverted four times and melted after each inversion to assure complete homogeneity. The amperage of melting was adjusted to prevent overheating. Very little loss due to evaporation was noted in each case.

D. THERMAL ANALYSIS

The use of the Knudsen effusion apparatus as a thermal analysis tool in addition to vapor-pressure analysis provided the means to determine the equilibrium phase diagram of the praseodymium-neodymium system without building a separate piece of equipment. The thermal analysis procedure is incorporated in with that of the vapor-pressure measurements.

The procedure used during a thermal analysis run was as follows. The temperature of the furnace was increased slowly at a rate of about 15°C per minute by an automatic drive mechanism, which controls the rotation of the furnace power Variac. The mechanism is a variable-speed transmission, manufactured by Graham Transmission, Inc. The time intervals were read off by one operator, and the temperature measurement was then taken by another operator. The temperature was varied through the solid-state transformations and the solidus and liquidus boundaries in both heating and cooling. This cycle was repeated several times until several data points were established for each heat effect. The data were plotted, and the arrests and inflections were determined from the graph. The accuracy of this measurement is ±5°C up to 1500°C.

To increase the sensitivity of the thermocouple to the thermal effects of a specimen, the bead was spot-welded in the upper corner of the thermocouple well by the spark-discharge technique. This intimate association with the solid or liquid contained inside the crucible provides a very accurate measure of the heat changes both during solid-state transformations and melting or solidification.

There is very little thermal lag in the temperature measurement. Even with small amounts of materials in the crucible, the thermal-analysis curves displayed very well-defined arrests or inflections, as the case may be.

E. X-RAY DIFFRACTION ANALYSIS

X-ray diffraction studies of the praseodymium-neodymium alloys as well as other rare-earth metals were made to determine the precise lattice parameters. The technique used was powder diffraction analysis of the alloy with a back-reflection film camera.

The preparation of the metal powder was done in an inert atmosphere in a dry box. A dry box was designed and built especially for this program. The dry box consists of an 8-inch-diameter cylindrical tube of transparent plastic. The tube is 12 inches long and is fitted with rubber-glove fittings at the two open ends. A connection to a vacuum source and an inert gas supply has been installed in the side wall of the tube. By alternately purging with inert gas and partially evacuating the dry box, an air-free atmosphere can be created. This condition is absolutely necessary to prepare uncontaminated filings of the rare earths. The filings were screened to -325 meash, wrapped in tantalum foil, sealed in evacuated quartz capsules, and annealed at 350°C for 24 hours to relieve the cold work. After the stress-relieving treatment, the powder was mixed in vaseline and placed on the specimen mount of the back-reflection camera.

The powder patterns were measured and analyzed using a linear least squares program on the Burroughs 205 digital computer. This technique followed the method of Cohen, in which the error is represented by $\phi \tan \phi$.

The back-reflection camera was calibrated with both high-purity potassium chloride and silicon. The silicon lattice parameters have been determined by two sources which show high accuracy. Vogel and Kempter[11] report the lattice parameter of silicon to be; $a = 5.4305 \pm 0.001$A. Swanson and Fuyat[12] report, $a = 5.4301 \pm 0.0001$A. A sample of Hyperpure silicon from Dupont de Nemours Company was subjected to precise back-reflection studies for comparison with the values in the literature. A lattice parameter, $a = 5.4303 \pm 0.001$A, was determined. The silicon was used as a calibration standard and as an internal standard with the rare-earth alloys.

F. KNUDSEN EFFUSION METHOD FOR VAPOR PRESSURES

Although the features of the Knudsen effusion method have been reported elsewhere,[13, 14, 15] it is briefly described below. The method determines the rate at which vapor effuses through a small orifice into a vacuum from a chamber in which the vapor is in steady-state equilibrium with the liquid or solid at a given temperature. The current study employs the gravimetric measurement technique

in which a fraction of the total molecules effusing through the orifice is collected on a target. The target, in turn, is suspended from an analytical balance. The weight of the vapor condensate deposited on the target is measured continuously from the time when the effusion cell reaches the pre-determined temperature until the time when the run terminates. One of the merits of this technique is the elimination of the error caused by heating-up and cooling-down times which is encountered in other techniques.

The form of Kundsen's equation used to calculate the vapor pressure is:

$$p = \frac{m}{Atf} \sqrt{\frac{2\pi RT}{M}} \qquad (1)$$

where p is the equilibrium vapor pressure in mm Hg, m is the condensed mass in g of the vapor with molecular weight M that effuses in t seconds through an orifice of cross-sectional area A in cm^2, T is the absolute temperature, and R is the molar gas constant in ergs per mole per degree. The factor f in the equation represents the fraction of effusing vapor that strikes the target and can be calculated from the cosine distribution law, assuming that the orifice acts as a point source, and that the length of the orifice is infinitesimally small compared to its radius. The following equation is used to calculate the factor:

$$f = \frac{r^2}{d^2 + r^2} \qquad (2)$$

where r is the radius of the target, and d is the distance from the effusion orifice of the Knudsen cell to the target.

Equation (1) is only valid under restrictive conditions. The mean free path of the molecule must be much greater than the dimension of the orifice. It is known experimentally that the ratio of the mean free path to the linear dimension of the hole must be at least 10.

The upper limit of the vapor pressure determined by the Knudsen effusion method is said to be about 0.01 mm Hg, while the lower limit is dependent upon the accuracy with which the amount of evaporated material may be determined.[14]

G. X-RAY SPECTROGRAPHIC ANALYSIS OF THE PRASEODYMIUM-NEODYMIUM SYSTEM

The accurate determination of the activities of the components of the praseodymium-neodymium binary alloy system requires the accurate determination of the relative amounts of each component deposited on the target in the Knudsen effusion apparatus. X-ray spectrographic analysis was selected as the

most convenient and accurate method for the amount of material involved in the individual determinations. Because of chemical similarity of the rare-earth elements, wet chemical methods were ruled out.

1. Standardization

Standard solutions were prepared to obtain calibration curves for the X-ray spectrographic analysis of the alloy vapors deposited on the target. Solutions were prepared by the following procedure. Arc melted alloys were used which contained 0 to 100 atomic percent neodymium in 10 percent increments. A 0.5 g sample of each alloy button was weighted on an analytical balance, placed in a 10 ml volumetric flask, and dissolved in nitric acid in the flask. After dissolution of the alloy the solution was diluted to 10 ml, and aliquots of each solution were mounted for X-ray analysis.

Two calibration curves were prepared. The total amounts of material on the sample mounts for the two curves were 10 and 15 mg. Each point on a curve was determined from the average fluorescent intensity of triplicate sample mounts rather than from a single sample mount. Precision volumetric glassware was used for all solution handling operations. Appropriate volumes of both neodymium and praseodymium standard solutions were pipetted onto the individual mounts to give the desired alloy composition and the desired total mass of material per mount.

The sample mount consisted of a circular plastic plug cap approximately 1 inch in diameter. A thin film mylar plastic was placed over the top of the plug cap and secured in place by a plastic lock ring. A disc of filter paper 1 inch in diameter was placed on top of the mylar film. The standard solutions were pipetted directly onto the filter paper. The solutions were evaporated to dryness, and a second mylar film was placed over the filter paper and secured in place by a second plastic lock ring. As a result of this procedure the sample was suspended in a sandwich of mylar film. The entire mount could then be placed in the X-ray unit for analysis.

2. Development of Technique

A 100-kv NORELCO spectrograph was used for instrumental examination of the prepared samples. This instrument was equipped with a tungsten-target X-ray tube, a lithium-fluoride analyzing crystal, 4 inches of 0.005-inch parallel blade collimation between the sample and the analyzing crystal, 2 inches of 0.005-inch parallel blade collimation between the analyzing crystal and the scintillation-counter detector, and associated electronic circuits for scaler measurements and recording of fluorescent X-radiation intensities.

Several techniques for study of the K spectra of praseodymium and neodymium with 100-kv excitation and the L spectra with 50-kv excitation can be

used. In consideration of resolution, line intensity, the binary system of adjacent elements in the periodic table, and other factors affecting the precise measurement of line intensities, a fixed-angle, fixed-time method was chosen with attention to a nominal value for precision in the range of ± 1 percent of the amount of the element present.

The region of the spectra for praseodymium and neodymium exhibiting the relative positions of the L lines for both elements is shown in Figure 6. The fixed-angle positions chosen for the two line-intensity measurements for each sample are indicated by "Pr" and "Nd" with the indicated two-theta angle values of 68.23 degrees for praseodymium and 65.06 degrees for neodymium. The X-ray tube was operated at 50 kv and 25 ma with intensity measurements for fixed-time intervals of 10 seconds each at the two-theta angle values indicated. Accuracy of the concentration values is dependent on the precision of results for measurement of the line intensity for each element in the sample and the precision of replication in sample preparation of the various aliquots. The factor of instrumental precision was evaluated by repetitive intensity measurements for the same sample. An overall average deviation from the mean of 0.4 percent was found for triplicate determinations in the 22 series of measurements with a maximum deviation of less than 1 percent. The individual intensity values are tabulated with calculated averages and percent deviations from the mean in Table IV. Triplicate samples were prepared containing the same quantity of each alloy. An indication of the accuracy of sample-mass replication was obtained by comparing measured line-intensity values for individual samples in the 22 groups of triplicates. The data and results are shown in Table V. The values of percent mean deviation include no consideration for instrumental precision. An average of 0.6 percent mean deviation is indicated for the overall precision of instrumental measurements and sample replication. Three values of mean deviation exceed 1 percent; however, in each case it is apparent that an individual sample in the group of triplicates is primarily responsible for the deviation from the average intensity value.

Concentration values for praseodymium and neodymium were determined for each sample by calculation of the average intensities for the triplicate aliquots. These values were used to prepare the standard reference calibration curves which are shown in Figure 7. The concentration values are tabulated in Table VI. The mean deviation is 1.5 percent on the basis of 100 percent composition for the total of both components of the binary system.

3. Preparation of Unknown Samples

The procedure for analyzing the unknowns was as follows. The target was removed from the Knudsen apparatus at the conclusion of each run, and the deposit was dissolved off using dilute nitric acid. The solution containing the deposit was evaporated to dryness, the residue dissolved in dilute nitric acid and made up to a

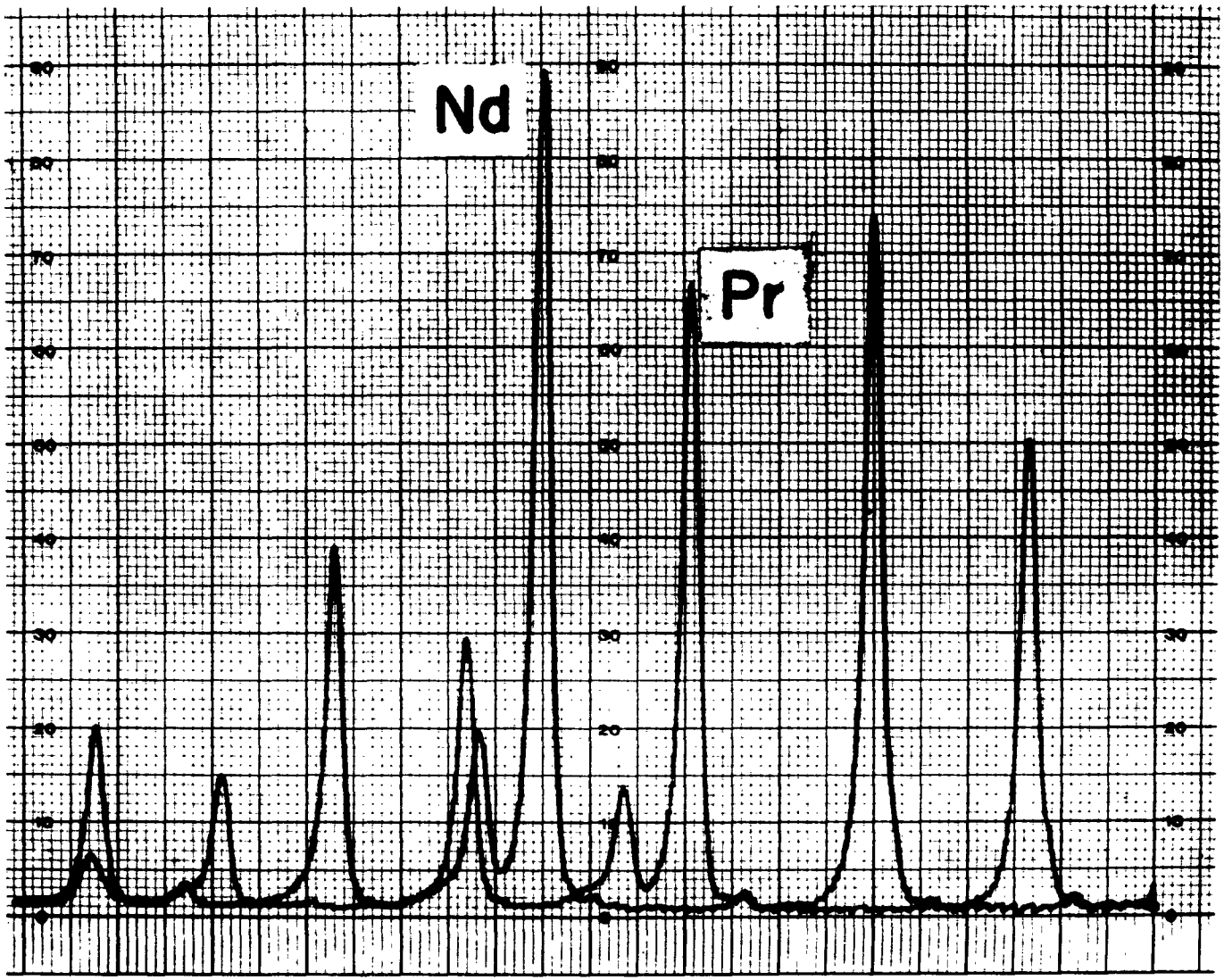

Figure 6. Fluorescence X-Ray Spectra of Praseodymium and Neodymium

TABLE IV

REPETITIVE INTENSITY MEASUREMENTS FOR SAME SAMPLE

Pr	Total Counts			Avg.	% Mean Deviation
100	55,424	55,680	55,552	55,552	0.15
90	49,152	49,792	49,280	49,408	0.52
80	45,904	45,776	45,904	45,861	0.13
70	37,760	37,376	37,504	37,546	0.38
60	33,024	33,152	33,024	33,066	0.17
50	27,520	27,392	27,264	27,392	0.31
40	21,504	21,888	21,760	21,717	0.65
30	17,152	16,896	16,896	16,981	0.67
20	11,264	11,264	11,392	11,306	0.50
10	6,016	5,888	6,016	5,973	0.95
0	---	---	---	---	---
Nd					
0	---	---	---	---	---
10	8,960	8,832	8,832	8,874	0.64
20	16,896	16,896	16,768	16,853	0.30
30	24,064	24,192	24,576	24,277	0.82
40	32,256	32,000	32,000	32,085	0.36
50	39,936	40,192	40,064	40,064	0.21
60	47,616	46,976	46,976	47,189	0.60
70	54,528	54,784	54,272	54,528	0.31
80	62,720	62,720	62,592	62,677	0.09
90	69,632	69,632	69,632	69,632	0
100	76,800	76,672	76,032	76,501	0.41

TABLE V

INDIVIDUAL INTENSITY MEASUREMENTS FOR TRIPLICATE SAMPLES

Pr	Total Counts			Avg.	% Mean Deviation
100	55,936	55,936	55,936	55,936	0
90	49,152	49,408	51,072	49,877	1.5
80	47,104	46,336	46,976	46,805	0.67
70	37,888	38,528	38,400	38,272	0.67
60	33,280	33,280	33,536	33,365	0.34
50	27,776	27,520	28,032	27,776	0.61
40	21,888	22,016	21,888	21,930	0.26
30	16,768	17,024	16,896	16,896	0.50
20	11,136	11,520	11,648	11,434	1.7
10	6,016	5,888	5,888	5,930	0.96
0	---	---	---	---	---
Nd					
0	---	---	---	---	---
10	8,704	8,960	8,960	8,874	1.3
20	16,896	16,640	16,768	16,768	0.45
30	24,064	24,192	24,192	24,149	0.24
40	32,128	32,128	31,872	32,042	0.36
50	40,064	39,936	40,192	40,064	0.21
60	46,720	47,104	46,720	46,848	0.37
70	55,040	54,784	54,272	54,698	0.52
80	62,336	62,976	62,336	62,549	0.45
90	70,016	69,376	69,504	69,752	0.42
100	77,056	76,160	75,904	76,373	0.60

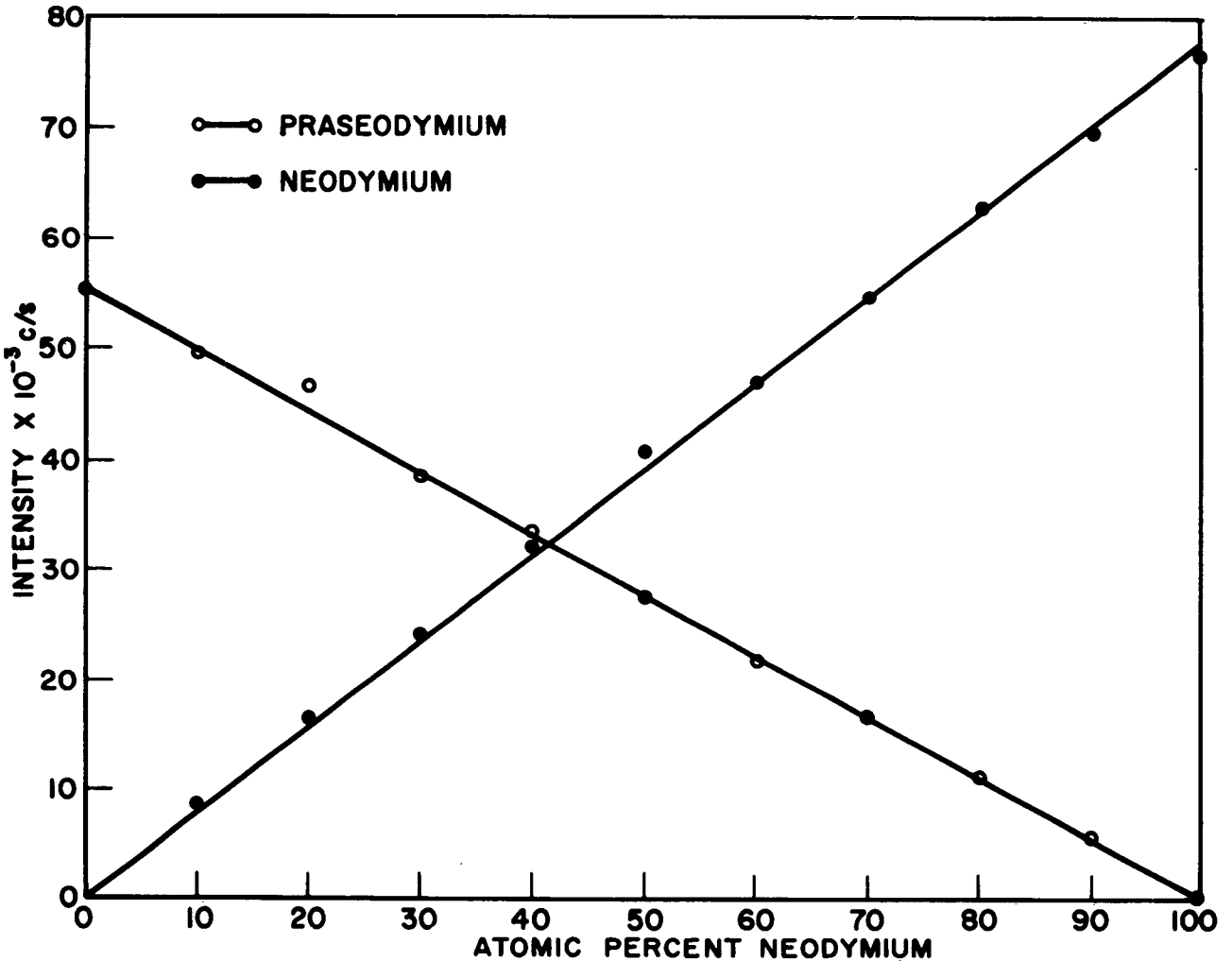

Figure 7. Standard Reference Calibration Curves for Praseodymium-Neodymium Alloys

TABLE VI

CONCENTRATION VALUES FOR PRASEODYMIUM-NEODYMIUM ALLOYS

Pr		Nd	
Nominal a/o	Actual a/o	Nominal a/o	Actual a/o
90	89.5	10	9.9
80	84.0	20	20.0
70	68.7	30	29.5
60	59.8	40	39.6
50	49.7	50	50.0
40	39.1	60	58.8
30	29.8	70	69.2
20	19.8	80	79.4
10	9.6	90	88.9

known volume, usually 10 ml. An appropriate portion of the 10 ml was then evaporated on an X-ray fluorescence mount, so that the total mass of material on the mount was 10 or 15 mg. The composition of these samples as determined by X-ray spectrographic analysis corresponded to the composition of the alloy vapor at the temperature of the determination.

H. METALLOGRAPHY

The preparation of surfaces of rare-earth metals or alloys for microscopic examination of their structure is difficult. Two principal problems are encountered. These are the formation of a surface free from reaction products (either from air contamination or the etchant) and from distrubed metal.

The specimens to be metallographically prepared were first cut from the arc-melted button with a jeweler's saw to prevent overheating and excessive working of the specimen. The piece was mounted in a cold-setting dental plastic which again does not require temperature and pressure to form as in the case of bakelite. Grinding was done slowly by hand using a solution of paraffin and Deobase (a purified kerosene) as a lubricant and coolant. The various stages of grinding include successive reductions in the size of the grit. The following silicon carbide grit sizes were used in the form of grit-bonded papers; 120, 240, 400, and 600 mesh. Polishing was accomplished with a Syntron Vibratory Polisher which polishes with a minimum of applied pressure. Two stages of polishing were employed. In the first, a slurry of Deobase and 5 micron alumina (Buehler AB #1) was used as the polishing medium. The Syntron Vibratory Polisher was operated at moderate amplitudes for 2-1/2 to 3 hours. The second and final stage of polishing was done with a slurry of 0.3 micron alumina and Deobase. The polisher was operated for 5 to 15 minutes.

All rinsing in between stages of grinding and polishing was done with Synasol (methyl alcohol). Water will form a reaction product on the surface if used.

Etching of all the rare-earth metals and alloys was accomplished with a mixture of glycerol and concentrated nitric acid. The composition found to be most generally acceptable was six parts of nitric acid to five parts of glycerol. The etchant was applied by thoroughly saturating a cotton swab and swabbing vigorously for 3 to 5 seconds. The specimen is immediately rinsed with profuse amounts of Synasol to stop the etching action. The etchant must be prepared immediately before using because the etchant deteriorates in several hours.

I. DENSITY MEASUREMENTS OF PRASEODYMIUM-NEODYMIUM ALLOYS

1. Room-Temperature Densities

(a) Displacement method. The density determinations of praseodymium, neodymium, and their binary alloys were made using the displacement method. The medium used was monobromobenzene which was purchased from Fischer Scientific Company. This certified reagent was calibrated against the variations in the ambient temperature with the aid of a copper-constantan thermocouple and a potentiometer by measuring the densities of super high-purity nickel (from Johnson, Matthey Co., Limited) and spectrographic grade tin (from Vulcan Materials Company) as standard materials.

Samples were weighed in air and in the bromobenzene on a Christian Becker Chain-o-matic analytical balance having an accuracy of ± 0.2 mg. In addition to the standard materials, the densities of spectrographic copper (from Johnson, Matthey Company, Limited), hyperpure silicon (from duPont Company), and semiconductor-grade germanium (from Sylvania Electric Products Company) were also determined as a check of the calibration.

(b) X-ray method. X-ray diffraction studies of the praseodymium-neodymium system have been made to determine the precise lattice parameters from which the X-ray densities of the alloys were determined. The technique used was a powder diffraction analysis of the alloy with a back-reflection film camera as described in a previous section.

2. Liquid Density Measurements

Modifications were incorporated into the Knudsen effusion apparatus to make possible the measurement of liquid densities of the praseodymium-neodymium alloys by the displacement method. The inside dimensions of the tantalum cell are 0.800 inch in height × 0.380 inch in diameter, providing a sufficient volume of liquid to completely immerse the cylindrical tantalum bob, measuring 0.188 inch in height × 0.188 inch in diameter. This bob was suspended by a 0.003 inch tantalum wire from the pan of the vacuum balance. The volume of the displaced liquid metal or alloy was determined from the weight loss of the immersed bob, correcting for the volume change of the bob due to expansion. A temperature of 1240°C was used for all of the liquid density measurements. Grooves of 0.005 inch were machined in the tantalum bobs to position the suspension wire. Calculations showed that the volume loss of the bob due to the machined grooves was compensated for by the volume of the wire immersed in the liquid metal.

Since the tantalum bob was not calibrated against any standard liquid metals, this method provides only relative values for the densities of the liquid alloys.

IV. RESULTS AND DISCUSSION

A. VAPOR-PRESSURE OF LIQUID SILVER

After the Knudsen effusion apparatus was designed and constructed, measurements of the vapor pressure of high-purity silver were undertaken to check the apparatus and technique. Silver was chosen as the comparative standard for the following reasons:

1) Various investigators have reported vapor-pressure data covering a wide temperature range.

2) These data are deemed reliable, especially those reported in recent years.

3) Silver of extremely high-purity is obtainable commercially.

4) Silver melts in the same relative temperature range as the rare earths under consideration.

5) Silver is convenient metal to work with because it is not prone to oxidize very readily, thus eliminating a source of error.

The investigation of the vapor pressure of liquid silver produced a series of data points in the temperature range from 1250 to 1397°K, which are tabulated in Table VII and are plotted in Figure 8 in terms of log p vs. 1/T. All the data points were obtained using the target method.

The temperature control of the Knudsen effusion cell was very satisfactory. The fluctuation of the cell temperature during the determination of silver vapor pressure was limited to ± 1°C, as detected with a platinum/platinum-13 percent rhodium thermocouple (B. & S. gage 28) and a precision potentiometer. The data published by other investigators, whose references are listed in Table VII, are incorporated in Figure 8. The data obtained by this investigation are in excellent agreement with those reported. It is noteworthy that Woolf, et al., [16] used the gas transportation technique for the vapor pressure study while McCabe and Birchenall[7] employed the method of weighing the effusion cell. The excellent agreement among these data, which were obtained with use of the diversified techniques, indicates that the accommodation coefficient experienced in this investigation was very close to unity.

The target temperature is rather critical for ideal accommodation of the vapor atoms that strike and condense to form nuclei. If the temperature is too high, the atoms re-evaporate causing a decrease of the accommodation coefficient. Yang, Simnad, and Pound[17] report that the accommodation coefficient of silver impinging on silver was measured to be unity at a target temperature not exceeding 200°C.

TABLE VII

VAPOR PRESSURE DATA OF LIQUID SILVER

Run No.	Temperature, °C	Time, seconds	Weight of Condensate g	Vapor Pressure mm Hg
13	977.6	25,800	0.0012	4.631×10^{-3}
11	1026.4	14,520	0.0039	1.086×10^{-2}
12	1050.5	18,330	0.0073	1.668×10^{-2}
15	1063.2	5,520	0.0016	2.979×10^{-2}
10	1077.6	10,785	0.0065	2.550×10^{-2}
7	1100	6,450	0.0062	4.100×10^{-2}
14	1107	6,600	0.0032	5.062×10^{-2}
9	1124	4,560	0.0065	5.888×10^{-2}

Legend to Figure 8:

J. Fischer, Z. anorg. u. allgem. Chemie, 219 (1934) 367-375.

H. von Wartenberg, Z. anorg. u. allgem. Chemie, 56 (1908) 320.

P. L. Woolf, G. R. Zellars, E. Foerster, and J. P. Morris, Report Investigations 5634, Bureau of Mines, 1960.

C. L. McCabe and C. E. Birchenall, Trans. AIME, 197 (1953) 707.

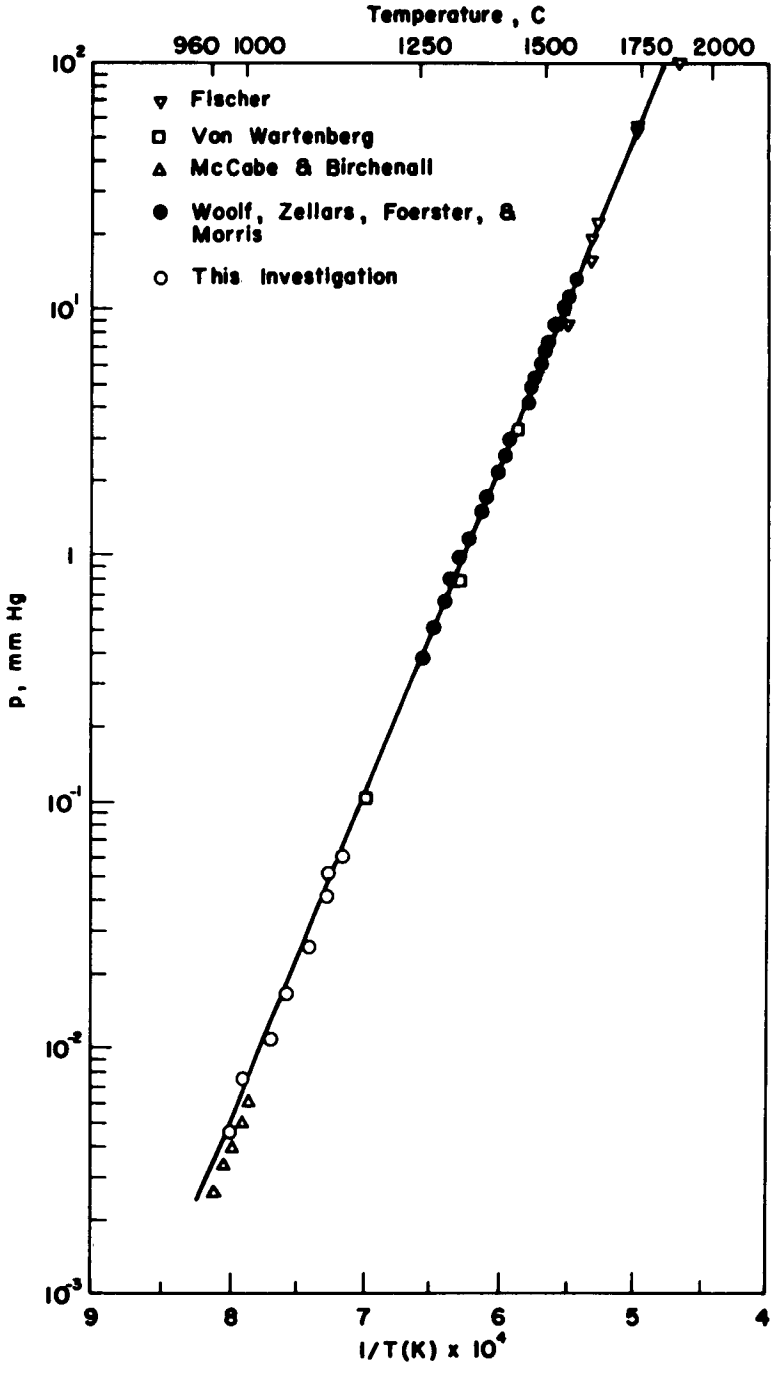

Figure 8. Plot of $\log_{10}$ p(mm Hg) vs. 1/T for Liquid Silver

Therefore, a cursory study of the target temperature in the experimental temperature range for the liquid silver, vapor-pressure determination was made at several different crucible temperatures. Two types of targets were investigated; one was pyrex glass and the other was sterling silver. The pyrex target reached a temperature of 165°C with a cell temperature of about 1000°C. On the other hand, the silver target reached a lower temperature of about 150°C in the same duration when the effusion cell was maintained at 1010°C. This indicates that the silver target is cooler than the target made of pyrex glass and did not seem to exceed 200°C in the temperature range up to 1100°C. This seems to validate the results obtained in this study.

B. THE PRASEODYMIUM-NEODYMIUM ALLOY SYSTEM

1. Phase Diagram

The phase diagram of the praseodymium-neodymium system was studied by metallographic, thermal analytical, X-ray, hardness, and density techniques. The diagram is presented in Figure 9. Alloys were prepared in 10 atomic percent increments throughout the phase diagram. The system exhibits complete liquid and solid solubility. The two solid-state forms of praseodymium and neodymium, namely the low-temperature hexagonal close-packed and the high-temperature body-centered cubic lattices, both exhibit complete miscibility.

The hardness data of the pure components and their alloys are presented in Table VIII. In summary, these data show very little hardness change in the alloys from one component to the other. Negligible solid solution hardening effects are present. The density data obtained for the binary alloys are presented in the subsequent section.

Metallographic examination of the as-cast alloys by 10 atomic percent increments established that the room-temperature allotrope is a continuous solid solution. Figures 10, 11, and 12 are the microstructures of praseodymium, neodymium, and a 50-50 alloy, respectively. The 50-50 alloy is representative of the microstructures observed in the other alloys also. The small particles of the dark phase are the oxide inherent in the material as-received from the Ames Laboratory of the U. S. Atomic Energy Commission. The metallographic techniques were described in an earlier section.

The thermal analysis of the components and the alloys was the most useful technique in establishing the phase diagram because it established the liquidus and solidus boundaries and also the temperature inflections of the boundaries involved in the transformation from the body-centered cubic form to the hexagonal close-packed form. The points establishing these boundaries can be seen in Figure 9.

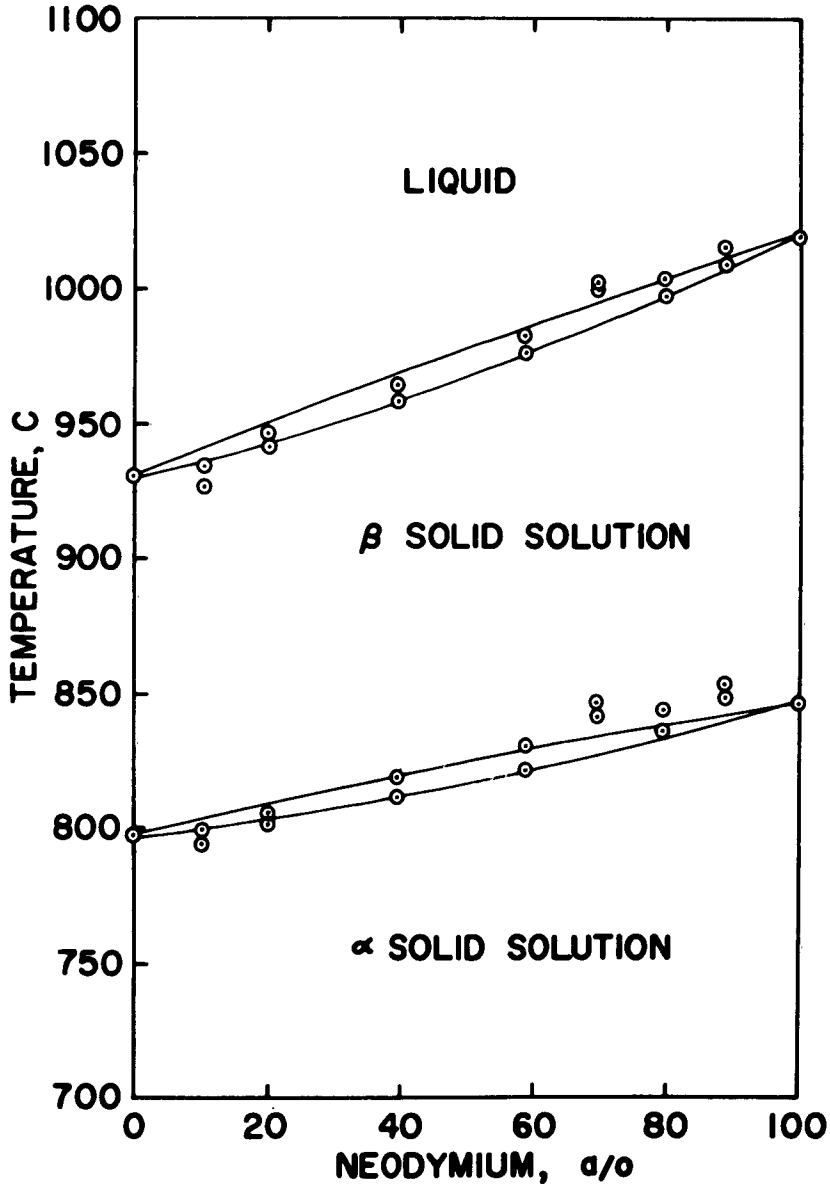

Figure 9. Phase Diagram of the Praseodymium-Neodymium System

TABLE VIII

HARDNESS DATA ON PRASEODYMIUM, NEODYMIUM AND THEIR ALLOYS

Alloy Composition, a/o	Melt No.	Hardness DPH, 2Kg Load
100% Pr	11	39.8
Pr-9.9% Nd	1	35.8
Pr-20.0% Nd	2	45.1
Pr-29.5% Nd	12	48.6
Pr-39.6% Nd	7	37.5
Pr-50.0% Nd	8	40.9
Pr-58.8% Nd	9	42.4
Pr-69.2% Nd	6	38.2
Pr-79.4% Nd	5	38.9
Pr-88.9% Nd	4	42.2
100% Nd	10	37.5
100% Pr, as-received	-	32.0
100% Nd, as-received	-	29.5
100% Pr	-	37*
100% Nd	-	35*

* C. E. Habermann, U. S. Atomic Energy Commission Publication 1959 (IS-15); the condition of the samples is given as "not annealed."

Figure 10. Structure of As-Received Praseodymium Metal

Figure 11. Structure of As-Received Neodymium Metal

Figure 12. As-Cast Structure of a Pr-50 Atomic Percent Nd Alloy

The procedure used in the thermal analysis experiments has been described in the experimental section. The data obtained in these experiments are tabulated in Tables IX, X, and XI.

The lattice parameters of praseodymium, neodymium, and their representative alloys were determined from the powder patters by the back-reflection camera method. The results are tabulated in Table XII and are plotted in Figure 13. The linear changes in the lattice constants, a and c, indicate that a continuous solid solution exists in the low-temperature crystalline form across the binary system. Furthermore, the conformity to Vegard's law across the α-solid solution region is noteworthy since very few binary solid solutions are known to obey this law. It substantiates the very close similarity of the praseodymium and neodymium species.

The c/a ratio and atomic volumes are also plotted in Figure 13. Both of these relationships exhibit linearity throughout the α-solid solution region.

2. Density, Observed and X-Ray

The density data of praseodymium and neodymium and their binary alloys were obtained employing the X-ray and displacement methods. The room-temperature density values are tabulated in Table XIII, together with those of the reference metals measured at the same time. As can be observed, the determined densities of the pure metals are in excellent agreement with those found in the literature. Also, there is very close agreement between the densities of the alloys as determined by the displacement and X-ray methods.

In general, the density, ρ, of a metal is related to the atomic volume, V° by the expression $V^\circ = M/\rho$ where M is the atomic weight of the metal. A quantitative study of the solid solution therefore may be made using the concept of the partial molal volume.[18] The linear relationship observed in the density-composition plot can be translated into linear volume changes in composition. The molal volume of an alloy, V, can be expressed as follows:

$$V = N_1\overline{V}_1 + N_2\overline{V}_2 \qquad (3)$$

where N_1, N_2 and V_1, V_2 are mole fractions and partial molal volumes, respectively, of the metallic components 1 and 2. By definition, $N_1 + N_2 = 1$.

Thus,
$$V = N_1\overline{V}_1 + (1-N_1)\,\overline{V}_2$$

$$= N_1(\overline{V}_1-\overline{V}_2) + \overline{V}_2. \qquad (4)$$

TABLE IX

THERMAL-ANALYSIS DATA FOR PRASEODYMIUM

Run No.	Melting Temperature °C	Freezing Temperature °C	Phase Transformation Temperature °C
1	---	930.5	795.0
2	---	---	795.0
3	929.8	930.0	795.8
4	---	931.3	---
Average		930.4	795.3
Reported Values		918.9*	792.2*
		935 **	798 **

* Metals Handbook, Vol. 1, 8th Edition, 1961, American Society for Metals, p. 1230.

** The Rare-Earth Metals, by F. H. Spedding and A. H. Daane, Metallurgical Reviews, Vol. 5, No. 19, 1960, Institute of Metals, p. 307.

TABLE X

THERMAL-ANALYSIS DATA FOR NEODYMIUM

Run No.	Melting Temperature °C	Freezing Temperature °C	Phase Transformation Temperature °C
1 (heating)	1020.1	---	844.0
(cooling)	---	1017.9	850.0
2 (heating)	1019.2	---	844.0
(cooling)	---	1018.5	850.0
Average		1018.9	847.0
Reported Values		1024±5*	862.2**
		1018.9**	862+

* A. H. Daane, Chapt. V, p. 413 in Progress in Nuclear Energy, Vol. 1, Ser. V, Pergamon Press, New York, 1956.

** Metals Handbook, Vol. 1, 8th Edition, 1961, American Society for Metals, p. 1230.

+ F. H. Spedding, A. H. Daane, K. W. Herrmann, Trans. AIME, 209 (1957) 895.

TABLE XI

THERMAL-ANALYSIS DATA FOR PRASEODYMIUM-NEODYMIUM BINARY ALLOYS

Nominal Alloy Composition Nd, a/o	Analyzed Nd Content a/o	Melting or Freezing Temperature Range °C	Transition Temperature Range °C
10	9.9	934.0 - 927.0	799.3 - 794.5
20	20.0	948.2 - 939.3	806.5 - 801.8
		947.0 - 941.0	806.0 - 801.0
40	39.6	964.0 - 958.0	818.0 - 811.8
		963.0 - 955.0	814.3 - 806.2
60	58.8	982.5 - 976.5	831.2 - 822.3
70	69.2	1002.0 - 999.0	846.5 - 842.0
80	79.4	1003.0 - 996.0	844.0 - 836.5
90	88.9	1015.0 - 1009.0	853.6 - 848.4

TABLE XII

Lattice Parameters of Praseodymium, Neodymium and Their Alloys

Alloy Composition a/o	Lattice Constants, A a_0	Lattice Constants, A c_0	Axial Ratio c/a	Atomic Volume cm^3
100 Pr	$3.6715_2 \pm 0.0007_5$	$11.8354_1 \pm 0.0027$	3.224	20.80
Pr- 20.0Nd	3.6690 ± 0.0008	11.8270 ± 0.0029	3.223	20.76
Pr- 29.5Nd	$3.6670_5 \pm 0.0004$	$11.8247_8 \pm 0.0017$	3.225	20.73
Pr- 50.0Nd	$3.6646_6 \pm 0.0005$	$11.8181_5 \pm 0.0019$	3.225	20.70
Pr- 69.2Nd	$3.6620_8 \pm 0.0004$	$11.8106_1 \pm 0.0019$	3.225	20.65
Pr- 88.9Nd	$3.6587_7 \pm$ —	$11.8030 \pm$ —	3.226	20.60
100 Nd	$3.6566_6 \pm 0.0005$	$11.7983_8 \pm 0.0026$	3.226	20.57
α-Pr*	3.6725 ± 0.0007	11.8354 ± 0.0012	3.223	20.82**
α-Nd*	3.6579 ± 0.0003	11.7992 ± 0.0005	3.226	20.59**

* F. H. Spedding, A. H. Daane, K. W. Herrmann, Acta Cryst., 9 (1956) 599.

** K. A. Gschneidner, Rare Earth Alloys, Van Nostrand Co., Inc., New York, 1961, p. 12

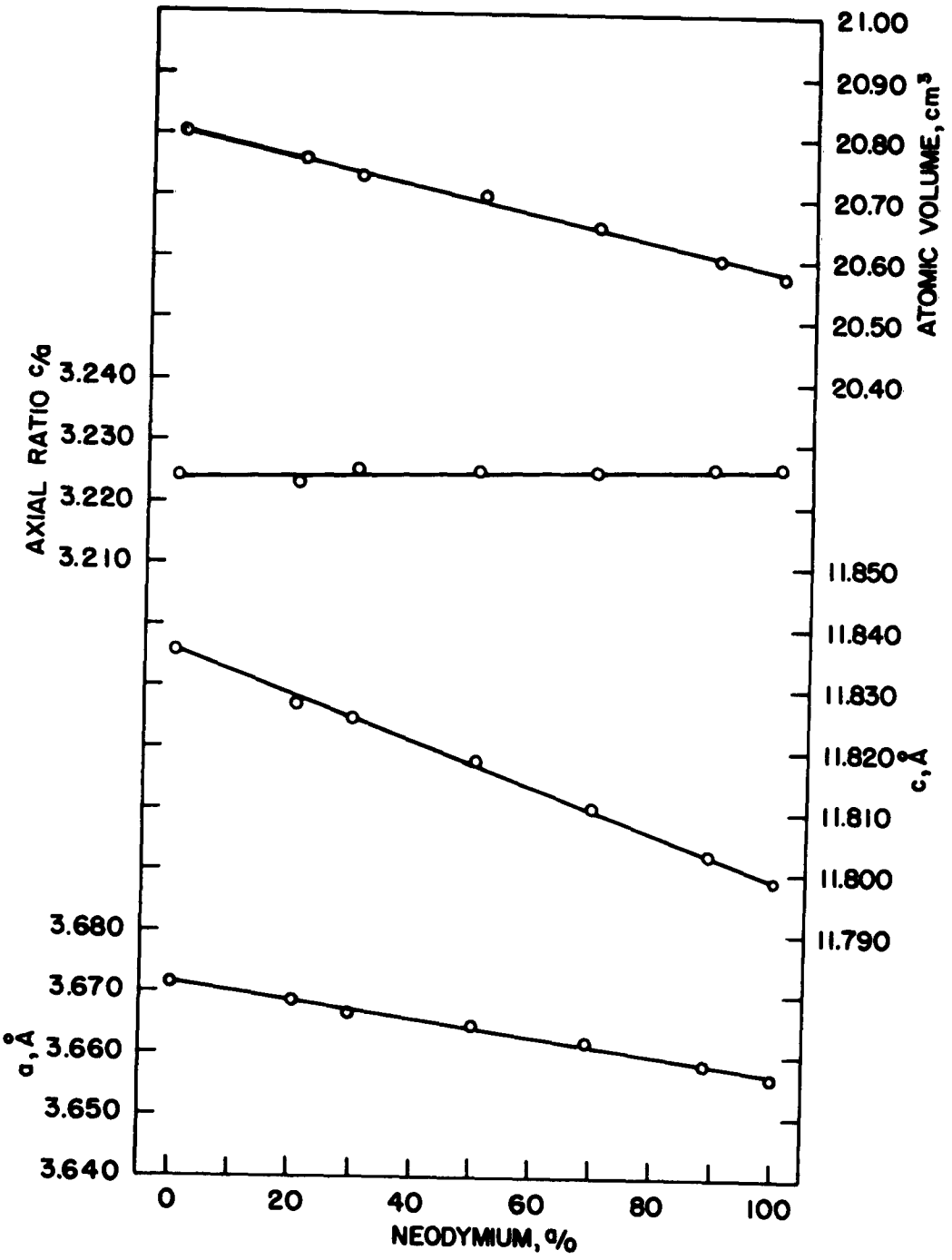

Figure 13. X-Ray Parameters vs. Composition for Praseodymium-Neodymium Binary Alloys

TABLE XIII

ROOM-TEMPERATURE DENSITY DATA OF PRASEODYMIUM, NEODYMIUM AND THEIR ALLOYS

Metals and Alloys	Analyzed Nd Content, a/o	Density, g/cc		
		Observed	X-ray	Literature
100 Pr (α-phase)	--	6.772	6.774	6.769 (X-ray)*
Pr - 10 a/o Nd	9.9	6.793	6.789	
Pr - 20 a/o Nd	20.0	6.816	-	
Pr - 30 a/o Nd	29.5	6.840	6,844	
Pr - 40 a/o Nd	39.6	6.858	-	
Pr - 50 a/o Nd	50.0	6.887	6,889	
Pr - 60 a/o Nd	58.8	6.908	-	
Pr - 70 a/o Nd	69.2	6.931	6.935	
Pr - 80 a/o Nd	79.4	6.958	-	
Pr - 90 a/o Nd	88.9	6.981	-	
100 Nd (α-phase)	-	7.005	7.012	7.007 (X-ray)*
Spectrographic Cu		8.949		8.96 (at 20°C)**
Semiconductor-grade Ge		5.321		5.323 (at 25°C)**
Hyperpure Si		2.327		2.33 (at 0°C)**

* F. H. Spedding, A. H. Daane and K. W. Herrmann, Acta Cryst., 9 (1956) 599.

** Metals Handbook, V. 1, 8th Ed., 1961, American Society for Metals, pp. 44-45.

If the solution is ideal, then $\overline{V}_1 = V_1^\circ$ and $\overline{V}_2 = V_2^\circ$, since $V_1^\circ = \frac{M_1}{\rho_1}$ and $V_2^\circ = \frac{M_2}{\rho_2}$, where M_1 and M_2 are atomic weights for components 1 and 2, respectively. Then by substitution of these in Eq (4), the following expression is derived for an ideal solution:

$$V = N_1 \left(\frac{M_1}{\rho_1} - \frac{M_2}{\rho_2} \right) + \frac{M_2}{\rho_2} \tag{5}$$

$\frac{M_1}{\rho_1}$ and $\frac{M_2}{\rho_2}$ are constant, and consequently the above equation expresses a straight-line relation between V and N_1. Assigning the appropriate values for N_1, M_1, M_2, ρ_1, and ρ_2, a series of the values for V can be obtained.

Now the molal volume of an alloy can be calculated by using the experimentally observed alloy density, ρ_A, and by assuming the average atomic weight of the alloy in the following manner,

$$N_1M_1 + N_2M_2 = N_1(M_1-M_2) + M_2. \tag{6}$$

Therefore,
$$V = \frac{N_1(M_1-M_2) + M_2}{\rho_A} \tag{7}$$

A plot of density versus atomic percent (mole fraction) is presented in Figure 14 for the room temperature values of the praseodymium-neodymium system. The linearity of this plot is obvious. Thus, from the above treatment showing the interdependence of density and molal volume, and the criterion that an ideal solution exhibits no volume change on mixing, the low-temperature phase of the praseodymium-neodymium system is essentially an ideal solid solution. The thesis of ideality in the system can be further supported by the linear relationship observed in the atomic volume vs. mol fraction plot (see Figure 13). The atomic volumes were calculated from the X-ray parameters.

In Table XIV are given the liquid densities of praseodymium, neodymium, and several of their binary alloys at a temperature of 1240°C. When these liquid densities were plotted against the alloy composition in atomic percent, a straight line relationship was also obtained, as in the case of the room-temperature densities (see Figure 14).

The linearity observed in the density vs. atomic percent plots for the binary system indicates that an ideal solution exists in both the room-temperature and liquid phases of the praseodymium-neodymium system.

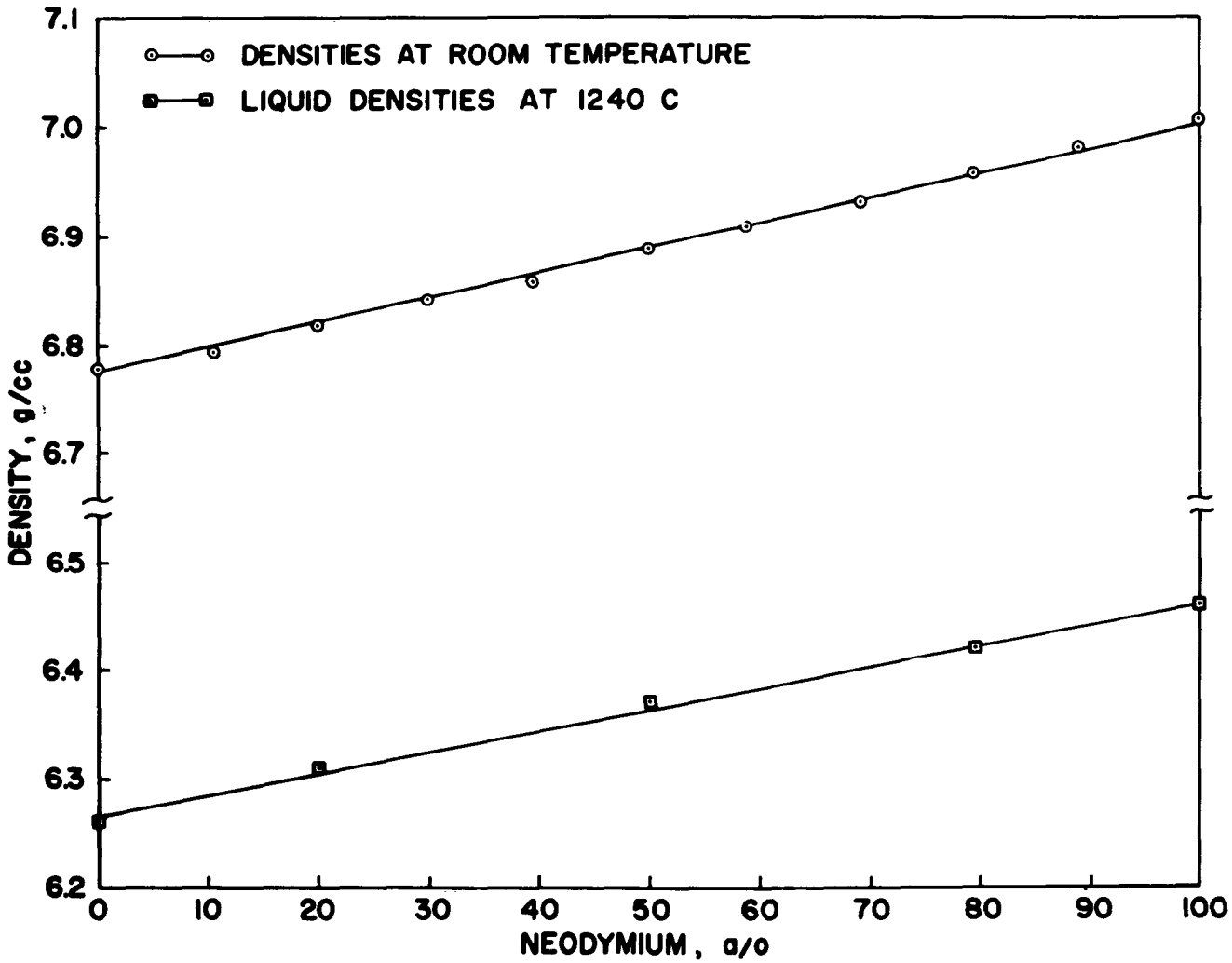

Figure 14. Density vs. Atomic Percent Plot for Praseodymium-Neodymium System at Room Temperature and 1240°C

TABLE XIV

Liquid-Density Data of Praseodymium, Neodymium and Their Alloys at 1240°C

Metals and Alloys	Analyzed Nd Content, a/o	Observed Density, g/cc
100 Pr	-	6.27
Pr - 20 Nd	20.0	6.31
Pr - 50 Nd	50.0	6.37
Pr - 80 Nd	79.4	6.42
100 Nd	-	6.46

There is excellent correlation between the liquid density studies and the results of the thermodynamic studies of the activities in the liquid, to be described later.

3. Vapor Pressures of Liquid Praseodymium and Neodymium

A literature survey of vapor-pressure data on praseodymium and neodymium reveals that no vapor-pressure determination of neodymium has been reported to date. The vapor pressure of praseodymium determined by the Knudsen effusion technique in conjunction with a quartz-fibre microbalance was reported by Daane[6] to be $\log_{10} p(\text{mm Hg}) = -17,188/T + 8.098$ in the temperature range, 1423 to 1693°K. This temperature range is below that required for this study. Therefore, it was deemed necessary to determine the vapor pressures of these two metals prior to the activity studies. The results obtained were published at the Second Conference on Rare Earth Research.[19]

Six vapor-pressure data points for liquid praseodymium in the temperature range from 1724 to 1874°K were obtained using the Knudsen effusion method. The species of praseodymium as well as neodymium were established to be monatomic by Johnson, et al.,[20] by mass-spectrometric measurements. Thus, the elemental atomic weights of the metals were used in the calculations. A least-squares treatment of the praseodymium vapor-pressure data gave,

$$\log_{10} p(\text{mm Hg}) = \frac{-18,450 \pm 425}{T} + 8.34 \pm 0.24.$$

Here, as in the following equation, p represents the pressure in mm of Hg and T, the temperature in degrees Kelvin. A plot of $\log_{10} p$ versus 1/T for praseodymium is shown in Figure 15. Two of the six points represent the vapor-pressure

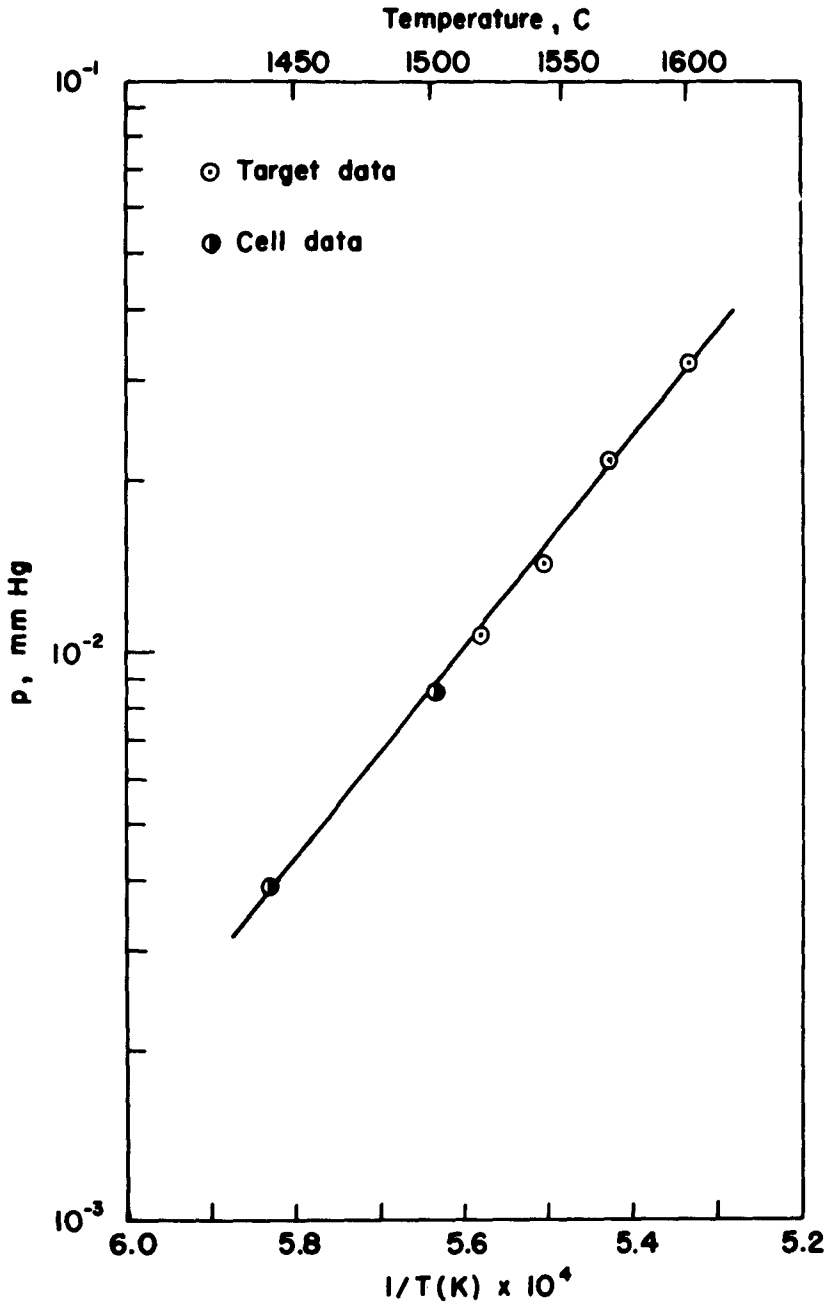

Figure 15. Plot of $\log_{10}$ P(mm Hg) vs. 1/T for Liquid Praseodymium

data which were calculated from the weight loss of the Knudsen cell. Agreement of these check points with the target data appears excellent, indicating an accommodation coefficient close to unity within the range of experimental errors.

Similarly, the vapor-pressure equation for liquid neodymium was established in the temperature range, 1638 to 1791°K:

$$\log_{10} p(\text{mm Hg}) = \frac{-18,375 \pm 500}{T} + 9.57 \pm 0.28$$

Twelve data points were determined for the metal, three points of which are direct weight-loss calculations of the Knudsen cell. Again, the accommodation coefficient is near unity. Figure 16 shows the straight-line plot for liquid neodymium. The standard deviations for the two constants in each equation shown above are in the order of ± 2.3 and 2.6 percent for praseodymium and ±2.8 and 2.9 percent for neodymium.

From the Clausius-Clapeyron relationship, the heat of vaporization was calculated from the slope of the curve for each metal. The heat of vaporization for praseodymium is 84.4 ± 1.9 kcal/mole, and the heat of vaporization for neodymium is 84.1 ± 2.2 kcal/mole. Since the reliability of the second law method is subjected to uncertainty due to inherent difficulties in determining the slope of the log p vs. 1/T plot accurately, the data were treated by the third law method to produce a value of ΔH°_{298}. However, the free energy functions for praseodymium vapor are not available, so that only the data for neodymium can be treated. The free energy functions necessary to calculate ΔH°_{298} were taken from Hultgren's compilation.[21] The derived ΔH°_{298} values by the third law method for neodymium are presented in Table XV and are also shown in Figure 17. The average ΔH°_{298} for neodymium is 76.2 ± 0.7 kcal/mole. The temperature consistency of each ΔH°_{298} value is evident in the above illustration.

Heats of vaporization for praseodymium and neodymium were calculated from mass-spectrometric studies by two other investigators. Johnson, et al.,[20] obtained values of 79.3 kcal/mole at 1380°K and 70.6 kcal/mole at 1348°K for praseodymium and neodymium, respectively, while White and his colleagues[22] obtained 71.4 kcal/mole at 1651°K and 71.1 kcal/mole at 1592°K, respectively. For easy comparison, White, et al., reduced the above values for neodymium to a common temperature of 298°K: ΔH°_{298} = 77.2 kcal/mole for their own and 75.0 kcal/mole for that of Johnson, et al. The ΔH°_{298} value obtained in this investigation, thus, compares favorably with the other two values cited above.

4. Activity Studies of the Praseodymium-Neodymium System

Speiser and St. Pierre[23] showed that it is not necessary to measure the vapor pressure of an alloy to determine the activities of its components. The

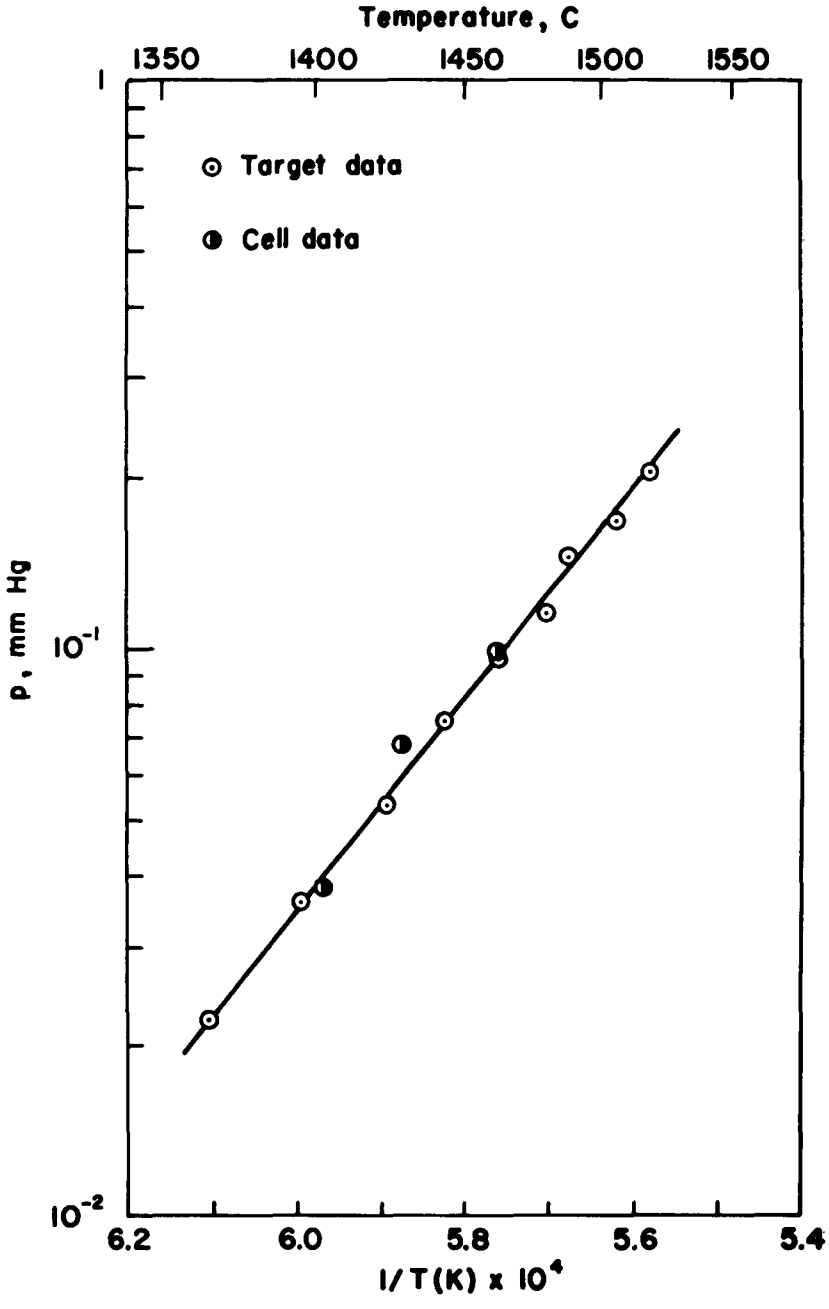

Figure 16. Plot of $\log_{10}$ P(mm Hg) vs. 1/T for Liquid Neodymium

TABLE XV

COMPUTATION OF THE HEAT OF SUBLIMATION OF NEODYMIUM, ΔH°_{298}, FROM VAPOR PRESSURE DATA

T, °K	-log p, atm	$-\left(\frac{F^{\circ}-H^{\circ}_{298}}{T}\right)^{*}_{gas}$	$-\left(\frac{F^{\circ}-H^{\circ}_{298}}{T}\right)^{*}_{solid}$	ΔH°_{298}, Kcal/mole
1638	4.534	50.69	24.47	76.9
1668	4.322	50.80	24.63	76.6
1675	4.296	50.82	24.68	76.7
1697	4.153	50.89	24.80	76.5
1701	4.047	50.90	24.82	75.9
1717	4.004	50.95	24.91	76.2
1736	3.888	51.02	25.02	76.0
1753	3.817	51.08	25.11	76.6
1761	3.716	51.10	25.15	75.6
1779	3.655	51.16	25.25	75.9
1791	3.570	51.19	25.31	75.6
			Average,	76.2

* From Hultgren's Compilation (21).

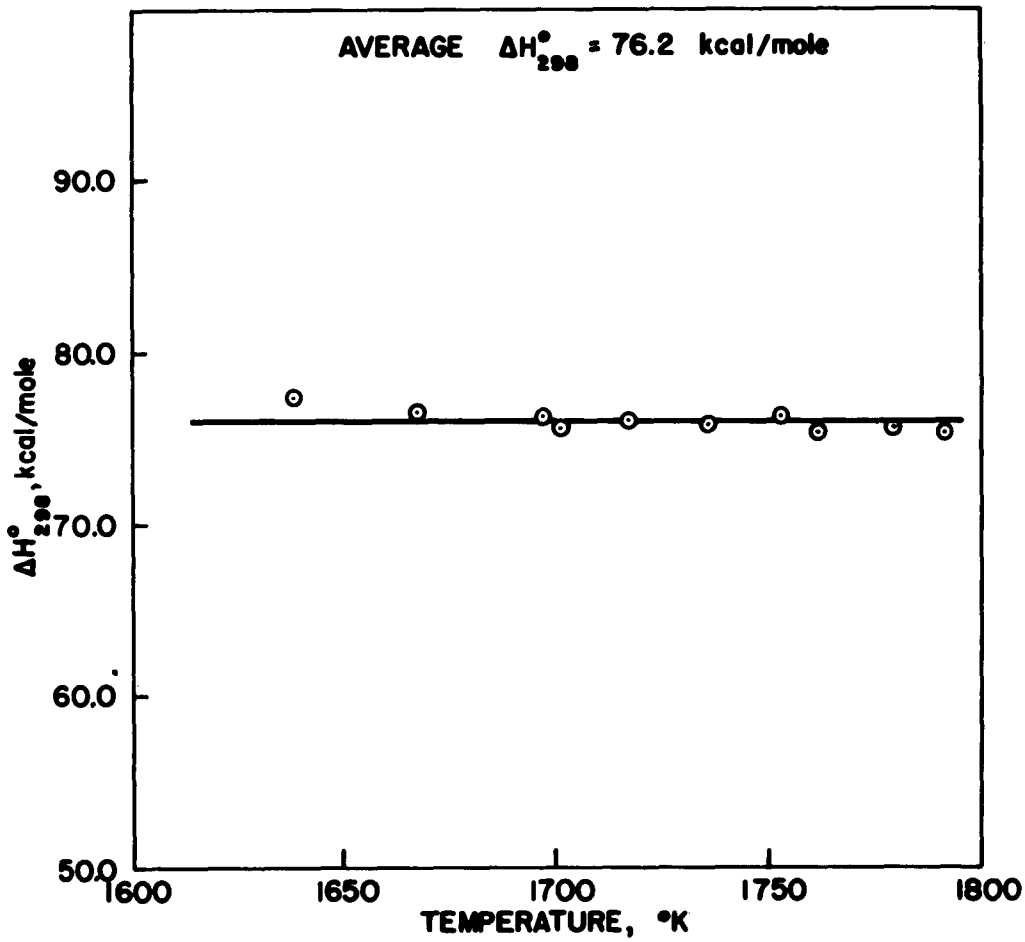

Figure 17. Plot of ΔH°_{298} vs. Temperature for Neodymium

activity of each component in the liquid alloy can be obtained by determining the ratio of the participating components in the condensed vapor phase. The application of a modified Gibbs-Duhem relation in determining the activities of iron and nickel in the liquid iron-nickel system was well demonstrated by Speiser, et al.[9] Their data were corroborated by Zellars, et al.,[24] who also determined the activities of iron and nickel by the use of the gas transportation method in which the vapor pressures of the alloys were directly measured. If it is assumed that the vapor of the alloy behaves as an ideal gas, the activity of component "i" is obtained with the following expression:

$$a_i^l = a_i^v = \frac{f_i}{f_i^0} \approx \frac{P_i}{P_i^0}$$

where the superscripts l, v and 0 refer to the liquid, the vapor and the pure component, respectively, and f and P represent the fugacity and pressure, respectively. The modified Gibbs-Duhem relation is,

$$\ln a_1^l = \ln \frac{P_1}{P_1^0} = \int_{N_1^v=1}^{N_1^v=N_1^v} \frac{N_2^l}{N_2^v} \, d \ln N_1^v$$

where the subscripts 1 and 2 represent the components, and N expresses the mole fractions of each component either in the vapor or liquid phase.

The activity determination in this investigation has been conducted using the modified Gibbs-Duhem relation as cited above. Each alloy was vaporized from a Knudsen effusion cell, and the condensate was collected on a cold target. The condensate was analyzed by an X-ray spectrographic technique. A more detailed description of the procedure appears in the experimental section. The analyzed compositions of the condensed vapor phases for a series of alloys at various experimental temperatures are tabulated in Table XVI in terms of their mole fractions.

(a) Praseodymium. The activities of praseodymium were calculated using the modified Gibbs-Duhem relation shown above. The values for a_{Pr}^l resulted from the graphical integration of a plot of N_{Nd}^l/N_{Nd}^v vs. $\ln N_{Pr}^v$, as shown in Figure 18, which represents the data obtained at 1500°C for praseodymium. Since the activities of praseodymium at 1475, 1500 and 1525°C are practically the same in this temperature range, the curve shown in Figure 17 is typical for all three temperatures.

TABLE XVI

CALCULATED ACTIVITIES FOR LIQUID PRASEODYMIUM AND NEODYMIUM ALLOYS

Run No.	N^l_{Nd}	N^l_{Pr}	Temperature, °C	N^v_{Nd}	N^v_{Pr}	a^l_{Nd}	a^l_{Pr}
127			1475	0.041	0.959	0.005	0.996
126	0.005	0.995	1500	0.031	0.969	0.003	0.994
125			1525	0.043	0.957	0.005	0.995
123			1475	0.469	0.531	0.099	0.904
122	0.105	0.895	1500	0.484	0.516	0.100	0.886
121			1525	0.490	0.510	0.095	0.898
103			1475	0.684	0.316	0.216	0.793
91, 104	0.200	0.800	1500	0.649	0.351	0.183	0.800
105			1525	0.658	0.342	0.176	0.809
87, 100			1475	0.834	0.166	0.336	0.616
89, 101	0.396	0.604	1500	0.836	0.164	0.390	0.590
102			1525	0.867	0.133	0.462	0.548
83, 110, 115			1475	0.912	0.088	0.584	0.432
111, 116	0.588	0.412	1500	0.912	0.088	0.565	0.409
117			1525	0.920	0.080	0.614	0.405
120			1475	0.947	0.053	0.734	0.302
119	0.692	0.308	1500	0.953	0.047	0.693	0.265
118			1525	0.943	0.057	0.712	0.321
77, 106, 109			1475	0.962	0.038	0.798	0.232
78, 107	0.794	0.206	1500	0.969	0.031	0.800	0.190
79, 108			1525	0.965	0.035	0.816	0.217
74, 98			1475	0.981	0.019	0.889	0.126
72, 97	0.889	0.111	1500	0.984	0.016	0.891	0.109
73, 99			1525	0.984	0.018	0.923	0.121

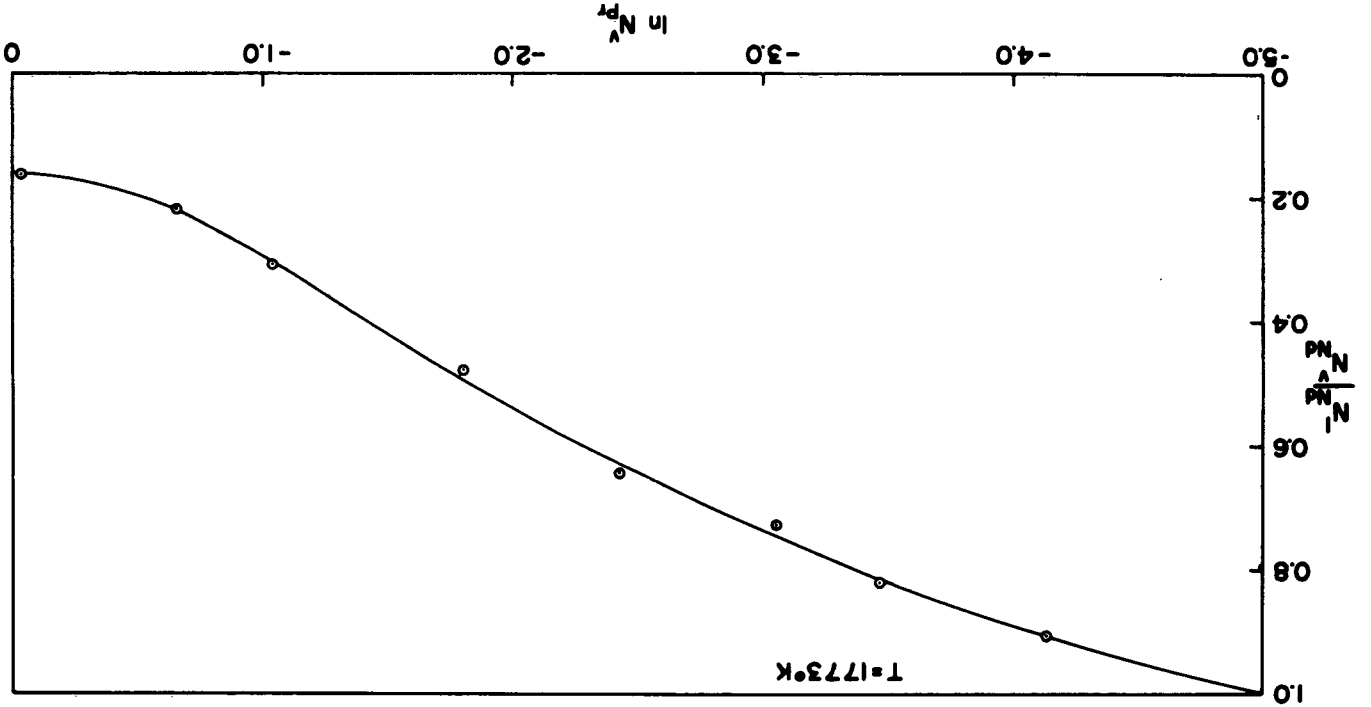

Figure 18. Plot of N^{l}_{Nd}/N^{V}_{Nd} vs. ln N^{V}_{Pr} at 1500°C

A graphical plot of a^l_{Pr} vs. N^l_{Pr} at 1500°C is shown in Figure 19. This is again typical of praseodymium for its activities at all three temperatures. As can be seen, the praseodymium demonstrates practically no deviation from ideality in the liquid phase of the praseodymium-neodymium alloy system. The calculated activities of praseodymium at various temperatures are included in Table XVI. No attempt was made to apply Graham's law correction to the activities because of the small difference between the molecular weights of praseodymium and neodymium.

(b) Neodymium. The determination of activities of neodymium in liquid praseodymium-neodymium alloys was based on the same method as described above for praseodymium. The activities of neodymium were determined for the liquid solutions at temperatures 1475, 1500 and 1525°C. The experimental data used for computing the activities are presented in Table XVI and Figure 20.

A plot of the activity versus mole fraction of neodymium at 1500°C is presented in Figure 19. The curves at 1475 and 1525°C are similar to that at 1500°C. Thus, there is negligible change in activity of neodymium in the liquid solution over the temperature interval measured. This condition parallels that of praseodymium which was described in the previous section. The neodymium exhibits essentially ideal behavior.

(c) Discussion. The praseodymium-neodymium system was selected as the first system of a series of binary systems to study the general alloying behavior of intra-rare-earth systems. The value of such a study was based on the enhanced ability to control the differences in properties of each component metal to a much closer degree than is possible with metals other than those in the lanthanide series. As pointed out in Section II, most of the rare-earth metals have properties which display practically a linear gradation with increasing atomic number. The crystal structures are very similar. Yet, there are enough differences in these properties to give a wide variety of combinations.

This program was initiated with a study of two component rare-earth metals which were chosen to be as similar in properties as could be obtained. Referring to praseodymium and neodymium in Table I, one sees that their crystal structures are identical, their Goldschmidt atomic radii and Pauling's single-bond radii are practically the same, their chemical valences are identical, and their electronegativities are the same. Thus, one would predict a very close approach to ideality in both the liquid and the solid solutions. The liquid and

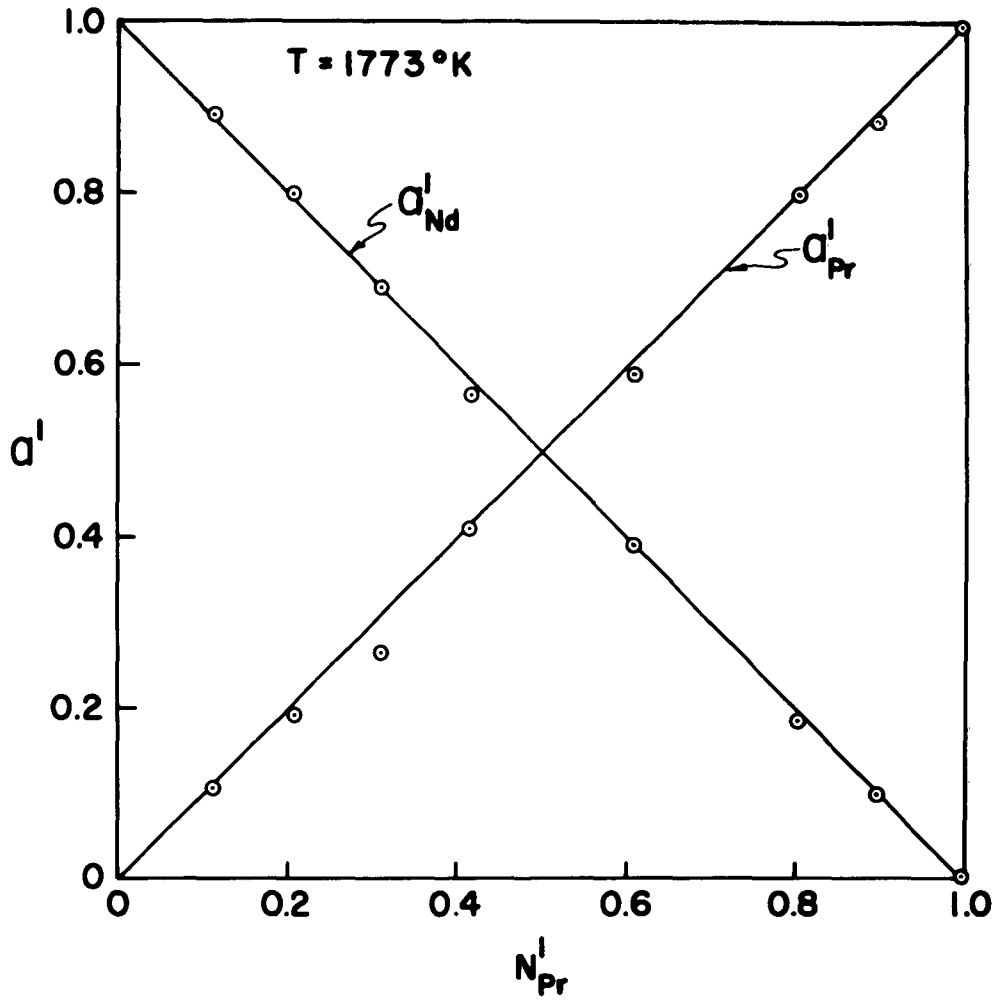

Figure 19. Plot of a^l_{Pr} and a^l_{Nd} vs. N^l_{Pr} at 1500°C

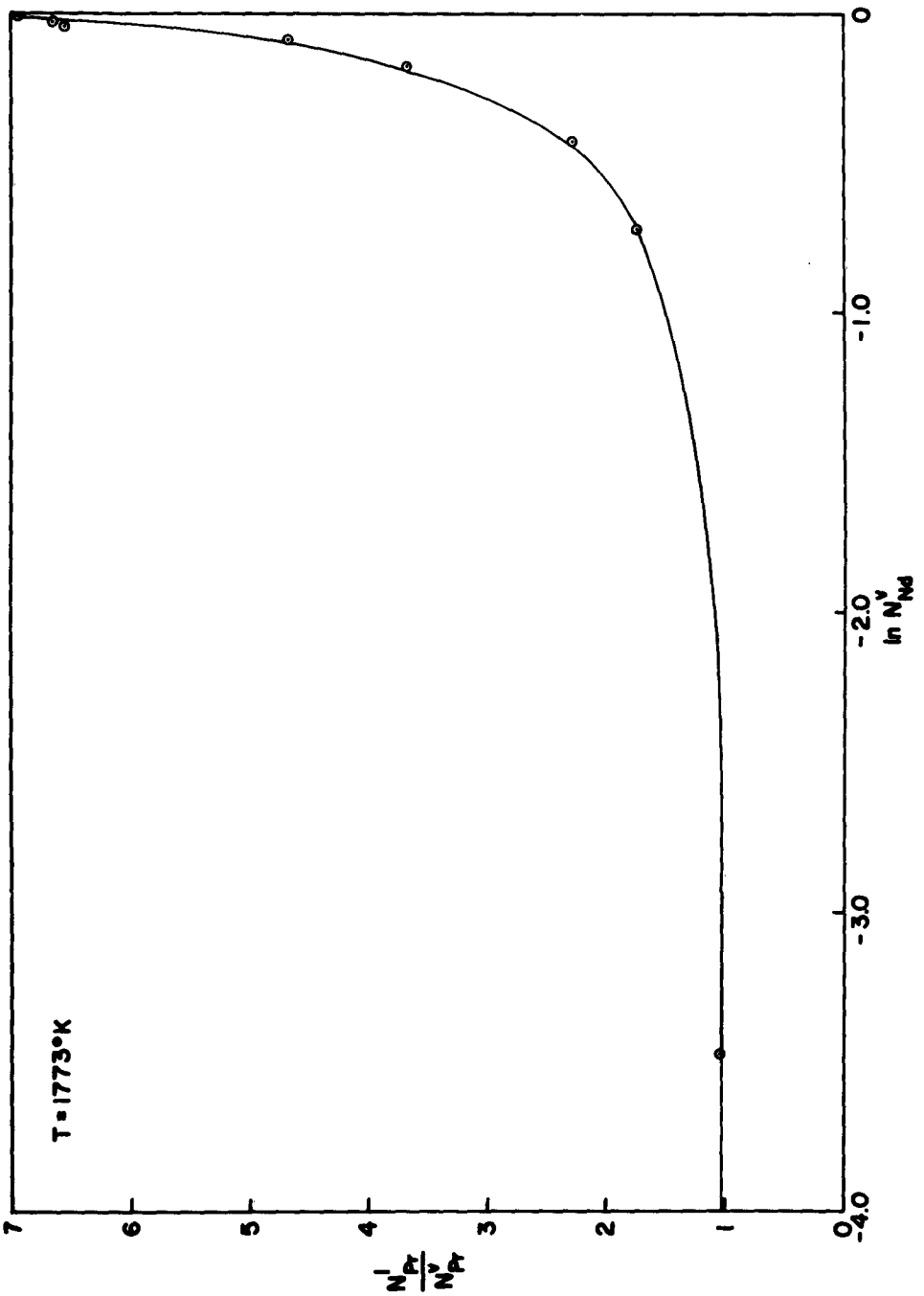

Figure 20. Plot of N^{l}_{Pr}/N^{v}_{Pr} vs. $\ln N^{v}_{Nd}$ at 1500°C

solid solution densities as determined by the displacement method and X-ray diffraction analysis exhibit no volume change on mixing one component with the other. This is one criterion for determining the conformity to ideality.

More conclusive of the approach of solutions of these two components to ideality is the thermodynamic activity data just described. Thus, the prediction of ideality on the basis of the similarities of praseodymium and neodymium is well established.

C. VAPOR PRESSURE OF SAMARIUM

Since there are no experimentally determined data available in the literature, a study of the vapor pressure of samarium was necessary. Determination of vapor pressures of both α-phase (low-temperature rhombohedral structure) and β-phase (cubic structure) was possible because of the rather high volatility of the metal. The direct weight loss method was employed. Seven data points were obtained in the low-temperature phase in the temperature range from 1033 to 1173°K while six points were determined in the high-temperature modification in the temperature range, 1202 to 1302°K. These data points are plotted as shown in Figure 21. A least-squares treatment of the vapor-pressure data for α- and β-samarium gives,

$$\log_{10} p_\alpha \text{ (mm Hg)} = \frac{-11,900 \pm 300}{T} + 9.71 \pm 0.24$$

$$\log_{10} p_\beta \text{ (mm Hg)} = \frac{-11,400 \pm 200}{T} + 9.30 \pm 0.21.$$

The heats of sublimation were calculated from the slopes of the above equations. For α-samarium the heat of sublimation is 54.5 ± 1.4 kcal/mole and for β-samarium, 52.3 ± 0.9 kcal/mole. Due to the inherent unreliability of the data produced by the second law method, the data were treated by the third law method to produce values of the heats of sublimation, ΔH°_{298}. The free energy functions necessary to calculate ΔH°_{298} were taken from Hultgren's compilation.[21] The calculated ΔH°_{298} values are presented in Table XVII. Figure 22 is a plot of these data versus the temperatures over which the data were generated, showing the consistency obtained by this method. The average ΔH°_{298} for α-samarium is 48.9 ± 0.4 kcal/mole and for β-samarium is 48.0 ± 0.5 kcal/mole. The difference between these two values is the heat of transition, ΔH_T, which is 900 cla/mole. The transition temperature of α- to β-samarium was determined by thermal analysis to be 911.5°C.

The only comparable data in the literature was reported by Savage, Hudson, and Spedding.[25] They determined the heat of sublimation of α-samarium

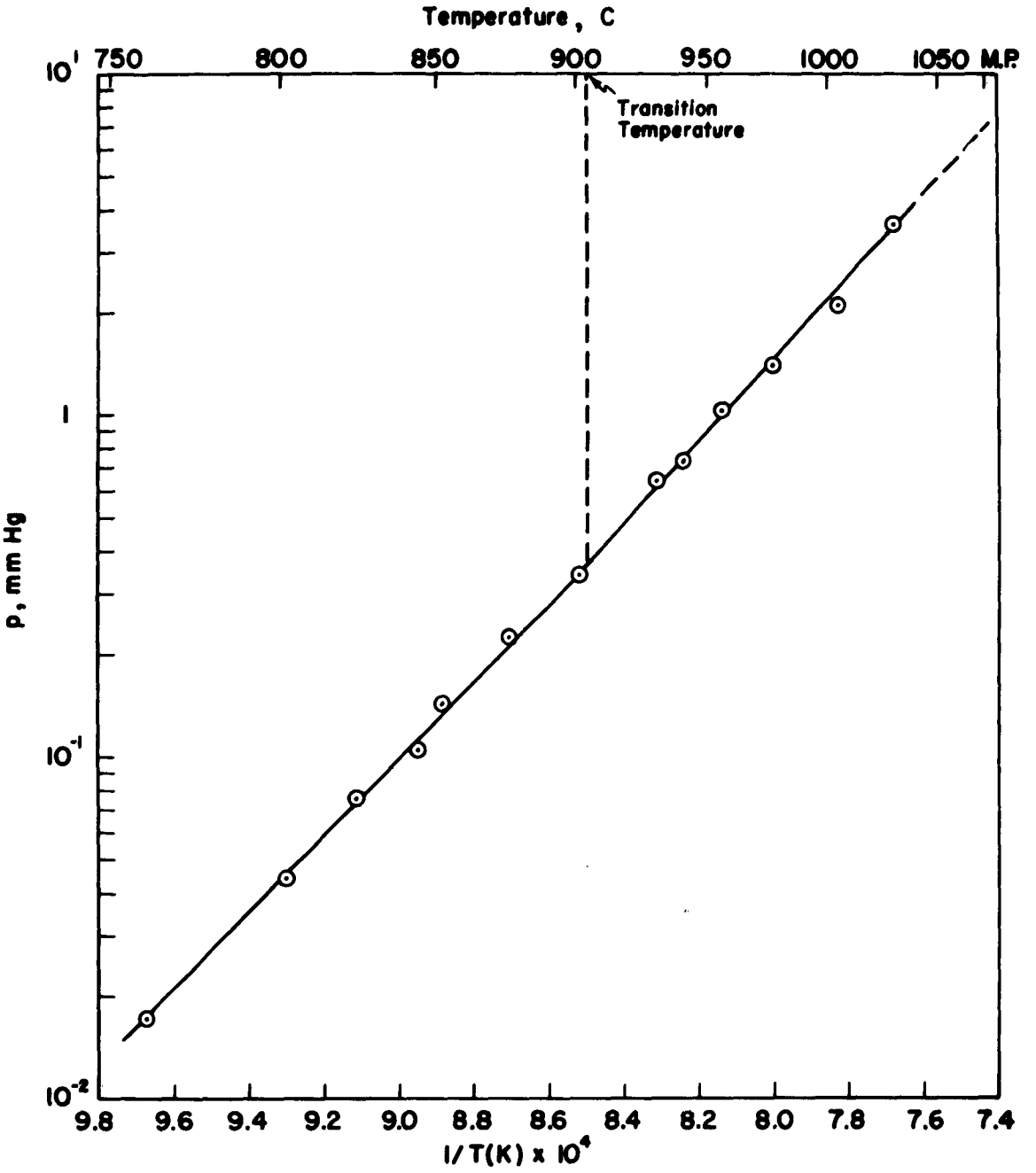

Figure 21. Plot of $\log_{10}$ p(mm Hg) vs. 1/T for α- and β-Samarium

TABLE XVII

COMPUTATION OF THE HEAT OF SUBLIMATION OF α- AND β- SAMARIUM, ΔH_{298}, FROM VAPOR PRESSURE DATA

T, °K	-log p, atm	$-\left(\frac{F^\circ - H^\circ_{298}}{T}\right)^*_{gas}$	$-\left(\frac{F^\circ - H^\circ_{298}}{T}\right)^*_{solid}$	ΔH°_{298}, Kcal/mole
α- Samarium				
1033	4.649	47.61	21.19	49.2
1075	4.234	47.82	21.46	49.1
1097	4.002	47.92	21.61	48.9
1117	3.852	48.02	21.74	49.0
1125	3.721	48.06	21.79	48.7
1148	3.526	48.17	21.94	48.6
1173	3.346	48.29	22.09	48.6
			Average,	48.9
β- Samarium				
1202	3.070	48.43	22.25	48.3
1213	3.015	48.48	22.33	48.4
1228	2.866	48.55	22.43	48.1
1243	2.738	48.61	22.53	47.9
1270	2.559	48.73	22.71	47.8
1302	2.319	48.88	22.91	47.5
			Average,	48.0

*From Hultgren's Compilation (21)

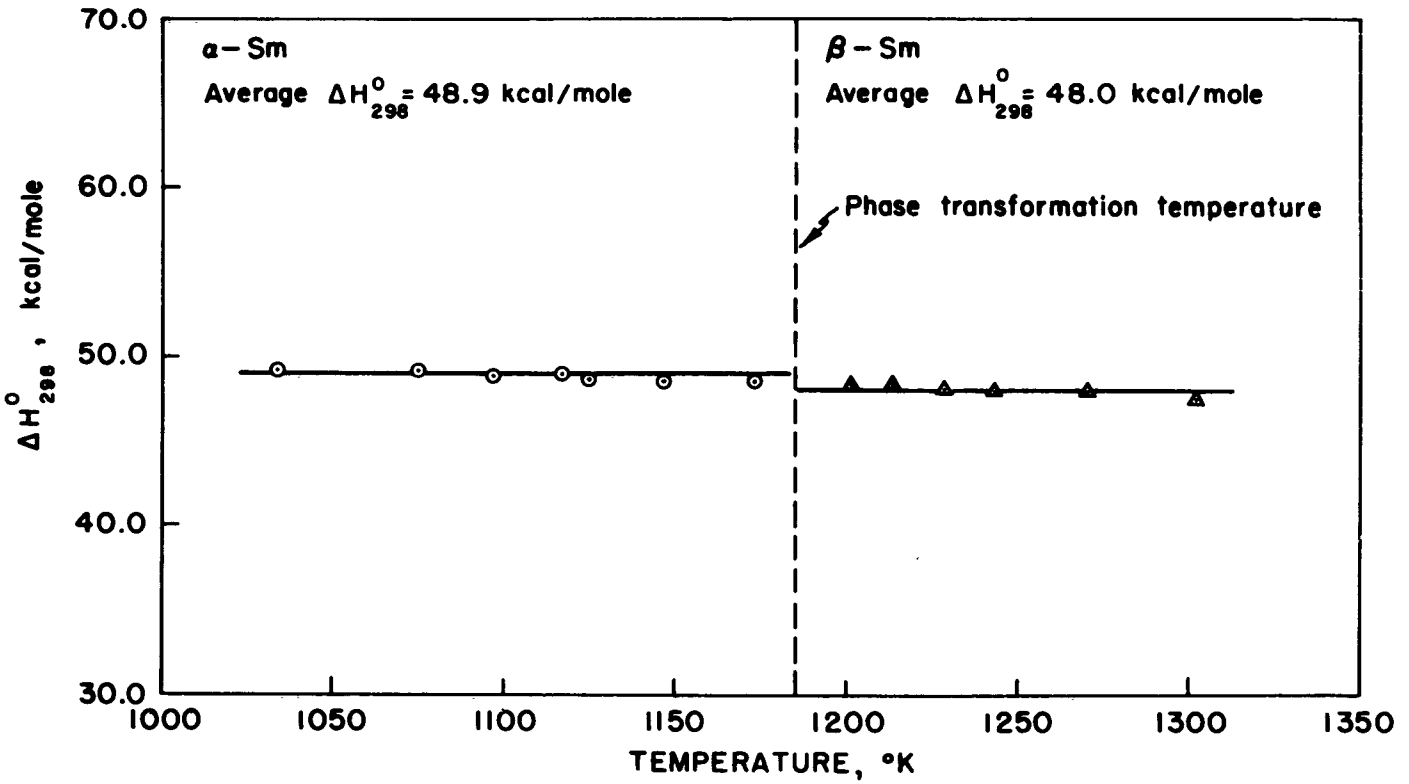

Figure 22. Plot of ΔH^{o}_{298} vs. Temperature for α- and β-Samarium

at 811°K, reporting $\Delta H° = 48.7 \pm 0.4$ kcal/mole. The technique they employed was mass spectrometric analysis of the vapor. No data have been previously reported on the heat of sublimation of β-samarium. The transition temperature of samarium was reported by Spedding, McKeown, and Daane [26] to be 917°C.

V. FUTURE CONSIDERATIONS

The research is presently being continued as outlined in Section II. This report describes only the initial phases of a broad program to study the alloying behavior of binary rare-earth systems.

REFERENCES

1. J. F. Smith, C. E. Carlson, and F. H. Spedding, Trans. AIME, 209 (1957) 1212.
2. L. Pauling, J. Am. Chem. Soc., 69 (1947) 542.
3. F. H. Spedding, J. J. Hanak, and A. H. Daane, Trans. AIME, 212 (1958) 379.
4. L. S. Darken and R. W. Gurry, Physical Chemistry of Metals, McGraw-Hill Book Co., New York, 1953, p. 80.
5. R. Speiser, A. J. Jacobs, and J. W. Spretnak, Trans. AIME, 215 (1959) 185.
6. A. H. Daane, AECD 3209, U. S. Atomic Energy Commission, Ames Laboratory, Ames, Iowa, 1950.
7. C. L. McCabe and C. E. Birchenall, Trans. AIME, 197 (1953) 707.
8. H. M. Schadel and C. E. Birchenall, Trans. AIME, 188 (1950) 1134.
9. J. C. Lachman and F. W. Knether, ISA Journal, April, 1960.
10. Metals Handbook, V. 1, 8th Edition, 1961, American Society for Metals, pp. 46-47.
11. R. E. Vogel and C. P. Kempter, Acta Cryst., 14 (1961) 1130.
12. H. E. Swanson and R. K. Fuyat, National Bureau of Standards Circular 539, 1953.
13. R. Speiser and H. L. Johnston, Trans. ASM, 42 (1950) 283.
14. R. Speiser and J. W. Spretnak, Vacuum Metallurgy, The Electrochemical Society, Inc., 1955, p. 155.
15. J. Chipman, J. F. Elliott, and B. L. Averbach, The Physical Chemistry of Metallic Solutions and Intermetallic Compounds, V. 1, Her Majesty's Stationary Office, London, 1959, Paper IB.
16. P. L. Woolf, G. R. Zellars, E. Foerster, and J. P. Morris, Report of Investigations 5634, Bureau of Mines, 1960.
17. L. Yang, M. T. Simnad, and G. M. Pound, Acta Met., 2 (1954) 470.
18. G. N. Lewis and M. Randall, Thermodynamics and The Free Energy of Chemical Substances, McGraw-Hill Book Co., New York, 1923, p. 33.
19. J. F. Nachman, C. E. Lundin, and A. S. Yamamoto, Proceedings of the Second Rare Earth Research, Gordon and Breach Science Publishers, New York, 1962, p. 163.

Aeronautical Research Laboratories, Wright-Patterson AFB, O. A FUNDAMENTAL INVESTIGATION OF THE ALLOYING BEHAVIOR OF THE RARE EARTH AND RELATED METALS by J. F. Nachman, C. E. Lundin, A. S. Yamamoto, University of Denver, Denver, Colo. January 1963. 68 p. incl. illus. tables. (Project 7021;Task 7021-01) (Contract AF 33(616)-6787) (ARL 63-15) Unclassified Report

The vapor pressures of praseodymium, neodymium and samarium have been measured with a Knudsen effusion apparatus. Also, using the same apparatus, thermodynamic activities of the liquid phase of the praseodymium-neodymium system have been determined. Heats of vaporization were established from the vapor pressure data for

(over)

UNCLASSIFIED

praseodymium, neodymium, and samarium. The phase diagram for the praseodymium-neodymium system was determined from thermal analyses, metallographic examinations and X-ray diffraction studies. Results of the thermodynamic activity studies and measurements of solid (room-temperature) and liquid densities indicate ideal behavior in both liquid and solid solutions, within the experimental error. Ideal behavior was predicted for the praseodymium-neodymium system, as there are essentially no difference between the component elements in considering such variables as electronic structure, crystal structure, atomic diameter, valency effect, electronegativity, and electron concentration.

UNCLASSIFIED

Aeronautical Research Laboratories, Wright-Patterson AFB, O. A FUNDAMENTAL INVESTIGATION OF THE ALLOYING BEHAVIOR OF THE RARE EARTH AND RELATED METALS by J. F. Nachman, C. E. Lundin, A. S. Yamamoto, University of Denver, Denver, Colo. January 1963. 68 p. incl. illus. tables. (Project 7021;Task 7021-01) (Contract AF 33(616)-6787) (ARL 63-15) Unclassified Report

The vapor pressures of praseodymium, neodymium and samarium have been measured with a Knudsen effusion apparatus. Also, using the same apparatus, thermodynamic activities of the liquid phase of the praseodymium-neodymium system have been determined. Heats of vaporization were established from the vapor pressure data for

(over)

UNCLASSIFIED

praseodymium, neodymium, and samarium. The phase diagram for the praseodymium-neodymium system was determined from thermal analyses, metallographic examinations and X-ray diffraction studies. Results of the thermodynamic activity studies and measurements of solid (room-temperature) and liquid densities indicate ideal behavior in both liquid and solid solutions, within the experimental error. Ideal behavior was predicted for the praseodymium-neodymium system, as there are essentially no difference between the component elements in considering such variables as electronic structure, crystal structure, atomic diameter, valency effect, electronegativity, and electron concentration.

UNCLASSIFIED